NAVAL POSTGRADUATE SCHOOL
Monterey, California

THESIS

Structural Considerations for Aircraft
Payload Modification-
P-3C Zero Fuel Weight Increase

by

Steven D. Culpepper
March 1991

Thesis Advisor: Edward M. Wu

Unclassified

Security Classification of this page

REPORT DOCUMENTATION PAGE

1a Report Security Classification Unclassified	1b Restrictive Markings
2a Security Classification Authority	3 Distribution Availability of Report
2b Declassification/Downgrading Schedule	Approved for public release; distribution is unlimited.
4 Performing Organization Report Number(s)	5 Monitoring Organization Report Number(s)
6a Name of Performing Organization: Naval Postgraduate School	6b Office Symbol (If Applicable) 67
6c Address (city, state, and ZIP code): Monterey, CA 93943-5000	7a Name of Monitoring Organization: Naval Postgraduate School
	7b Address (city, state, and ZIP code): Monterey, CA 93943-5000
8a Name of Funding/Sponsoring Organization	8b Office Symbol (If Applicable)
8c Address (city, state, and ZIP code)	9 Procurement Instrument Identification Number
	10 Source of Funding Numbers

Program Element Number	Project No	Task No	Work Unit Accession No

11 Title (Include Security Classification) STRUCTURAL CONSIDERATIONS FOR AIRCRAFT PAYLOAD MODIFICATION- P-3H ZERO FUEL WEIGHT INCREASE

12 Personal Author(s) Steven D. Culpepper,LT USN

13a Type of Report	13b Time Covered		14 Date of Report (year, month,day)	15 Page Count
Master's Thesis	From	To	March 1991	77

16 Supplementary Notation The views expressed in this thesis are those of the author and do not reflect the official policy or position of the Department of Defense or the U.S. Government.

17 Cosati Codes			18 Subject Terms (continue on reverse if necessary and identify by block number)
Field	Group	Subgroup	Aircraft structures, Center section wing box, Euler-Bernoulli, Finite Element model, Structural analysis

19 Abstract (continue on reverse if necessary and identify by block number

The Navy is considering the feasibility of increasing the patrol aircraft P-3C zero fuel weight enabling avionics and payload growth. This analysis examines the consequences to the structural requirements of the center section wing box. Two solutions to the structures field equations are investigated: a simplified hand solution for preliminary feasibility calculations and a more precise solution for design analysis. Together, the solutions provide a necessary check for the results. The simplified solution employs the Euler-Bernoulli assumption which generates a set of integrals expressed in terms of the assumed displacements. These integrals, when combined with simplified geometric shapes and symmetry, ultimately produce a decoupled matrix solution. The precise solution uses a PC based finite element method which simultaneously solves the field equations for basic elements to be linked together with the appropriate boundary conditions. For the current 135,000 pound gross weight 1g load condition, the internal stresses calculated by finite element are in accord with those by simplified hand calculation. Extensions from this modeling will generate design criterion for the target 95,000 pound zero fuel weight aircraft as well as alternate flight or taxi conditions.

20 Distribution/Availability of Abstract	21 Abstract Security Classification
[X] unclassified/unlimited [ ] same as report [ ] DTIC users	Unclassified

22a Name of Responsible Individual	22b Telephone (Include Area code)	22c Office Symbol
Edward M. Wu	(408) 646-3459	67

DD FORM 1473, 84 MAR 83 APR edition may be used until exhausted security classification of this page

All other editions are obsolete Unclassified

Approved for public release; distribution is unlimited.
Structural Considerations For Aircraft Payload Modification-
P-3H Zero Fuel Weight Increase.

by

Steven Drew Culpepper
Lieutenant, United States Navy
B.S., United States Naval Academy, 1983

Submitted in partial fulfillment of the requirements for the degree of

MASTER OF SCIENCE IN AERONAUTICAL ENGINEERING

from the

NAVAL POSTGRADUATE SCHOOL
March 1991

ABSTRACT

The Navy is considering the feasibility of increasing the patrol aircraft P-3C zero fuel weight enabling avionics and payload growth. This analysis examines the consequences to the structural requirements of the center section wing box. Two solutions to the structures field equations are investigated: a simplified hand solution for preliminary feasibility calculations and a more precise solution for design analysis. Together, the solutions provide a necessary check for the results. The simplified solution employs the Euler-Bernoulli assumption which generates a set of integrals expressed in terms of the assumed displacements. These integrals, when combined with simplified geometric shapes and symmetry, ultimately produce a decoupled matrix solution. The precise solution uses a PC based finite element method which simultaneously solves the field equations for basic elements to be linked together with the appropriate boundary conditions. For the current 135,000 pound gross weight 1g load condition, the internal stresses calculated by finite element are in accord with those by simplified hand calculation. Extensions from this modeling will generate design criterion for the target 95,000 pound zero fuel weight aircraft as well as alternate flight or taxi conditions.

TABLE OF CONTENTS

LIST OF FIGURES

ACKNOWLEDGMENTS

I am especially grateful to Professor Wu for his commitment to this undertaking and his friendship; Without either this project would never have flown. In addition I would like thank Professor Kwon for his invaluable assistance in the finite element arena.

I. INTRODUCTION

The Navy is considering the feasibility of increasing the patrol aircraft P-3C zero fuel weight enabling avionics and payload growth. An 18,000 pounds payload increase from the current zero fuel weight of 77,200 pounds will undoubtably require airframe structural modifications. This payload increase to the present configuration will accommodate system upgrades into the next century.

This analysis will provide the tools to determine whether the existing center section wing box can accommodate the additional loads or if a modification is required. Modification options ranging from variations of the existing geometry to materials substitution such as composites will be discussed.

A structural analysis, which provides a basis for strength and stability assessment, begins by modeling the geometry and boundary conditions of the center section wing box for a given flight condition. An idealized model constructed from rods and sheets replaces the center section wing box. This model approximates the geometry of the structure while providing a necessary simplification that facilitates the mathematical solution to the solid structures field equations. The wing boundary conditions are provided by a contractor while a component inventory method (Appendix A) is used to construct the fuselage loads.

Two solutions to the field equations provide a necessary check on the results. The Euler-Bernoulli assumption uncouples the field equations and leads to an integral representation of stresses in terms of the boundary condition resultant loads applied at the centroid. The idealized model geometry (Figure 1) allows the boundary value problem to be integrable thereby yielding a closed form of the solution. From this closed form, a solution to uniformly distributed (centroid) forces and moments is practical. The second solution uses the Finite Element Method (FEM) to simultaneously satisfy the field equations for basic elements or geometries. These elements are combined to form the structure of interest. This numerically based solution method allows a solution of more realistically distributed forces and moments as well as refined geometric configurations. The problem formulation and computational implementations for the current application are verified for the idealized

model using closed-form hand calculated results. The Saint Venant principle enables the resultant boundary condition loads to be modeled at the centroid thereby verifying the (lower bound) internal stresses predicted by the hand calculations for the static case. Upon verification of the hand calculated results, the finite element model may be used to examine various realistic inertial loadings within the center section wing box for any given flight condition in the operational envelope.

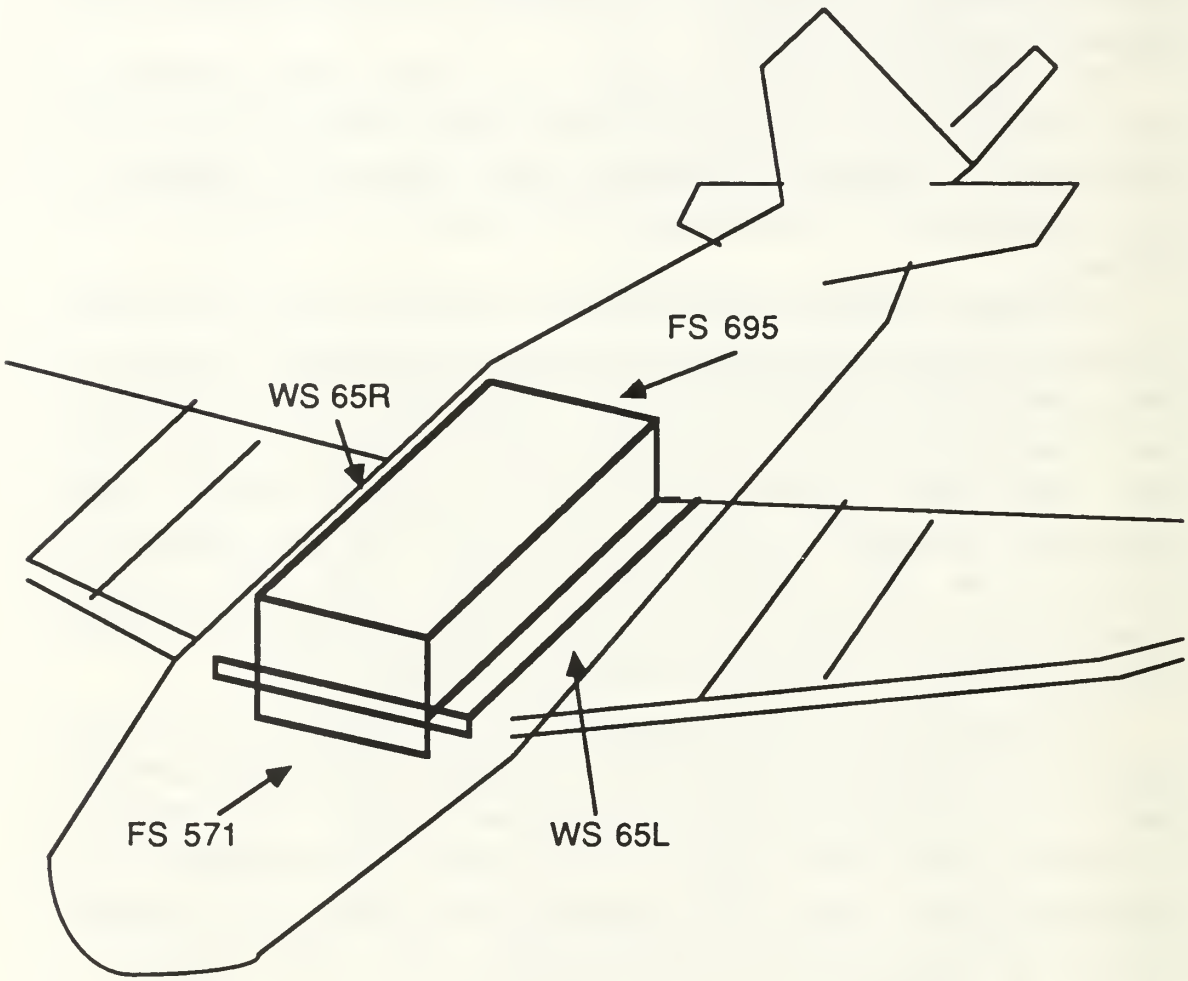

Figure 1. Idealization of the Center Section Wing Box: rod and sheet structure replace actual P-3 geometry to facilitate closed form of mathematical solution.

Validation of the boundary condition stresses generates confidence in the solution of the center section wing box for various inertial loadings. New boundary loads for the proposed flight conditions of interest will help

identify critical stress and deformation locations within the structure. The finite element software lends itself to parametric studies of alternative structural configurations in addition to exploring the effects of increasing the load requirements on the airframe from, for example, 3 to 3.5 g's. Other materials including composites may be examined as replacement options. New configurations can be readily analyzed by fine tuning the boundary load conditions. These benefits lead one to the utilities of this structural analysis. It provides a readily accessible feasibility check of the existing structure and a means to design alternatives for the center section wing box. The analytically generated data may form the basis for Request For Proposals (RFP) which may include innovative designs (ie. composites) and structural modifications.

II. Problem Definition

The future P-3 version H will accommodate an increase in the zero fuel weight from 77,200 to 95,000 LBS. The weight added will occur within the fuselage section of the aircraft. The proposed solutions to this structural problem include replacing the entire wing, and replacing all or strengthening weak members of the center section wing box. Each of these solutions requires an in-depth knowledge of the structural limitations of the current center section wing box. Specifically, the question remains whether the modified structure will support the added stress and strain given the increase in zero fuel weight.

A. BOUNDARY CONDITIONS

The worst case conditions for the center section at maximum gross weight include a 2g taxi bump on the ground and a sustained 3g turn in the air. The lift generated by the wings accelerate the 155,000 pound airframe with a load factor of 3.0. This lift transmits a moment and a shear into the center section at wing station 65 (refer to Figure 1) The forward and aft fuselage sections impart moments and shears into the center section fuselage stations 571 and 695 respectively. The taxi load is generated by the main landing gear impulses subjecting the inboard nacelles to vertical accelerations. While this condition delivers a shear, the moment is of opposite sign to the aerodynamic load yet it still acts on the center section at wing station 65. For purposes of this study, the 1g in-flight loading condition was analyzed in detail. Other loading conditions were provided to cover the full spectrum of situations.

B. FUSELAGE LOADS

The fuselage loads for a 135,000 pound aircraft were constructed using the data provided by the current P-3 version C Specification printed in 1982. The weights of various components (ie. wing, propulsion, body, tail, electronics etc.) were broken down into fuselage weight and wing weight both inboard and outboard of wing station 65. The fuselage weight was

then distributed along the airframe based upon the location of the components. The shear and moments were built up from this weight distribution and tabulated in Appendix A. The loadings along the center line of the fuselage were computed from:

$$M = n \sum_{i=1}^{m} w_i l_i \qquad (2.1)$$

$$V_Z = n \sum_{i=1}^{m} w_i \qquad (2.2)$$

$w_i \equiv$ weight of the i_{th} component

$l_i \equiv$ moment arm of the i_{th} component

$n \equiv$ load factor

$m \equiv$ number of components

The moment arms were referenced to F.S. 571 for the forward section and to F.S. 695 for the aft portion of the fuselage.

C. WING LOADS

The wing loads were provided by Aerostructures, Inc. located in Arlington, Virginia (Appendix A). Their data was extrapolated from values given for the eight loading conditions in Lockheed's Structural Life Extension Program report for the P-3C. The bending moment and shear were provided for 1g and delta 1g increments along the entire wing starting at the center line and continuing out to wing station 584. The load accuracy was quoted as between five and ten percent. The moment

contribution about the wing M_y is calculated as the shear multiplied by the distance between the lift line and mid-chord (approximately 0.2 chord).

A first order method to calculate the wing loads requires the lift to act through the center of pressure on the mean aerodynamic chord (Figure 2). This moment and shear felt at wing station 65 is countered by the weight of the wing and fuel (wet wing). The total moment and shear at W.S. 65 is determined by dividing the wing up into sections and summing the incremental shears and moments produced at W.S. 65 by the outboard lift distribution.

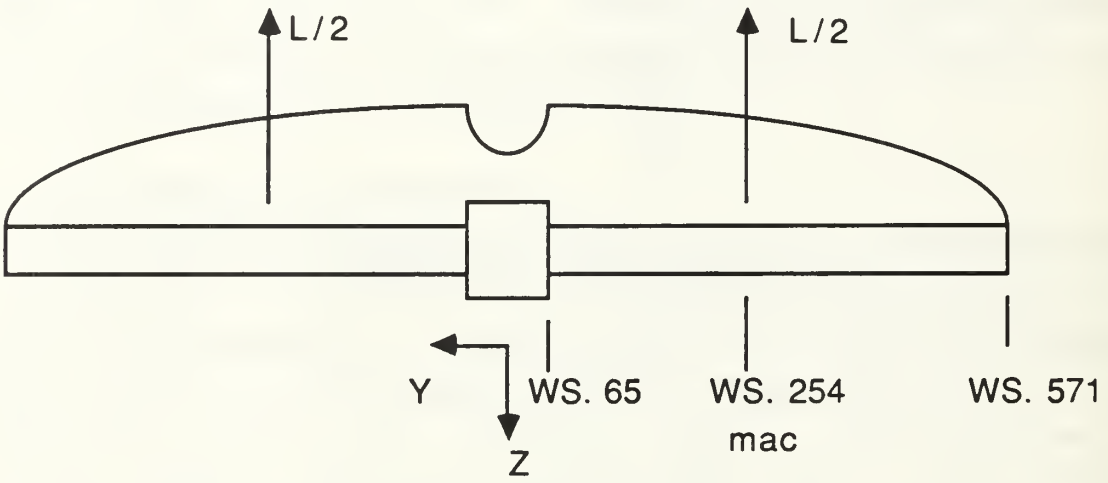

Figure 2. Two Dimensional Lift Distribution : simplified resultants (as seen by center section) shown at mean aerodynamic chord (mac).

D. GROUND TAXI LOADS

The ground taxi loads were provided by Mr Nam Phan (NAVAIRSYSCOM). The maximum gross weight condition occurs when the plane rolls over a 2g bump and the wing responds in a flexible manner. The gear through the inboard nacelle accelerate vertically upward while the fuselage and fuel ladened wing outboard of the nacelle resist the motion. The bending moment located at wing station 65 during this condition creates tension on the wing top and compression on the bottom.

E. CONTROL SURFACE LOADS

A rudder kick produces a torque about the fuselage, a moment about the vertical axis and an insignificant y-direction shear. The vertical distance from the rudder center of pressure to the longitudinal (x) axis multiplied by the lift produced by the rudder due to a deflection into the slipstream adequately describes the torque experienced by the fuselage. The moment generated by the rudder is a product of the rudder lift times the longitudinal distance from F.S. 695 to the rudder center of pressure.

Elevator deflection incrementally alters the shear and moment produced at F.S. 695. The elevator force directly adds to the remainder of the shear at F.S. 695. The control force was multiplied by the longitudinal distance measured from the elevator aerodynamic center to F.S. 695 to produce this moment. The moment was added with all the rest at F.S. 695.

Ailerons generate incremental amounts of lift in comparison to that produced by the remainder of the wing. As such, they can be readily incorporated into the calculations. The shear adds directly to that already calculated at W.S. 65. The moment results from the lifting force on the aileron acting about the moment arm established by the aileron center of pressure to W.S. 65.

This summary of load conditions exhausts the list that need be examined for purposes of structural integrity. These conditions should in fact be pared down further to a minimum set that can be quickly incorporated into the model and determine whether or not the structure has been overloaded. The answer to the overload question will determine the need for wing box redesign thereby closing the design loop.

III. GENERAL SOLUTION TO P-3C

The general engineering solution provides a linear analysis to the question raised regarding the P-3H structural response to an increase in zero fuel weight. This solution yields an essential comparison for the output of the finite element program as an accuracy check. This formulation is based on an assumed general form for the displacements with the parameters to be determined by the specific boundary conditions. This formulation reduced the solution of the field equations to algebraic forms (after the necessary integrations) thus bypassing the necessity of solving 18 partial differential equations simultaneously.

A. SOLUTION USING EULER-BERNOULLI ASSUMPTION

The assumed displacement method was originally used by Euler and Bernoulli over a century ago. Essentially, plane sections are assumed to remain plane during application of bending loads. The limitation to the theory lies in its application to only small deformations. Strain, defined in terms of the partial derivatives of displacement, can be calculated for the structure in terms of the assumed displacements. The constitutive relationship for a specific material (i.e. aluminum) converts the strain to internal stress. The internal equilibrium equations establish a set of equations in terms of integrals for solution in terms of internal stresses. These internal stresses are then equilibrated to the boundary tractions. A system of integral stress equations related to the known applied boundary conditions result. The solution of the integrals in this system of equations is further simplified through the idealization of the actual structural configuration by interconnecting bars (to carry normal stress) and sheets (to carry shear). The structure in Figure 3 models the center section wing box of the P-3C. The internal stresses within the individual members are constant permitting their extraction from the integrand thereby facilitating the integration, which results in a system of algebraic equations. The general solution, now represented in matrix form contains many coupling elements. Decoupling is accomplished through the application of symmetry

to the geometry and using the specific loads that apply for a particular flight condition. We note that this simplification is possible only for the simplified centroidal (uniformly loaded) boundary conditions. Nevertheless, this solution provides a useful estimate of the best case expectations (lower bound stress) and it also provides a bench mark verification for the finite element method solution which will be used for examination of the realistic cases in terms of payload distribution, structural modification and structural material substitution.

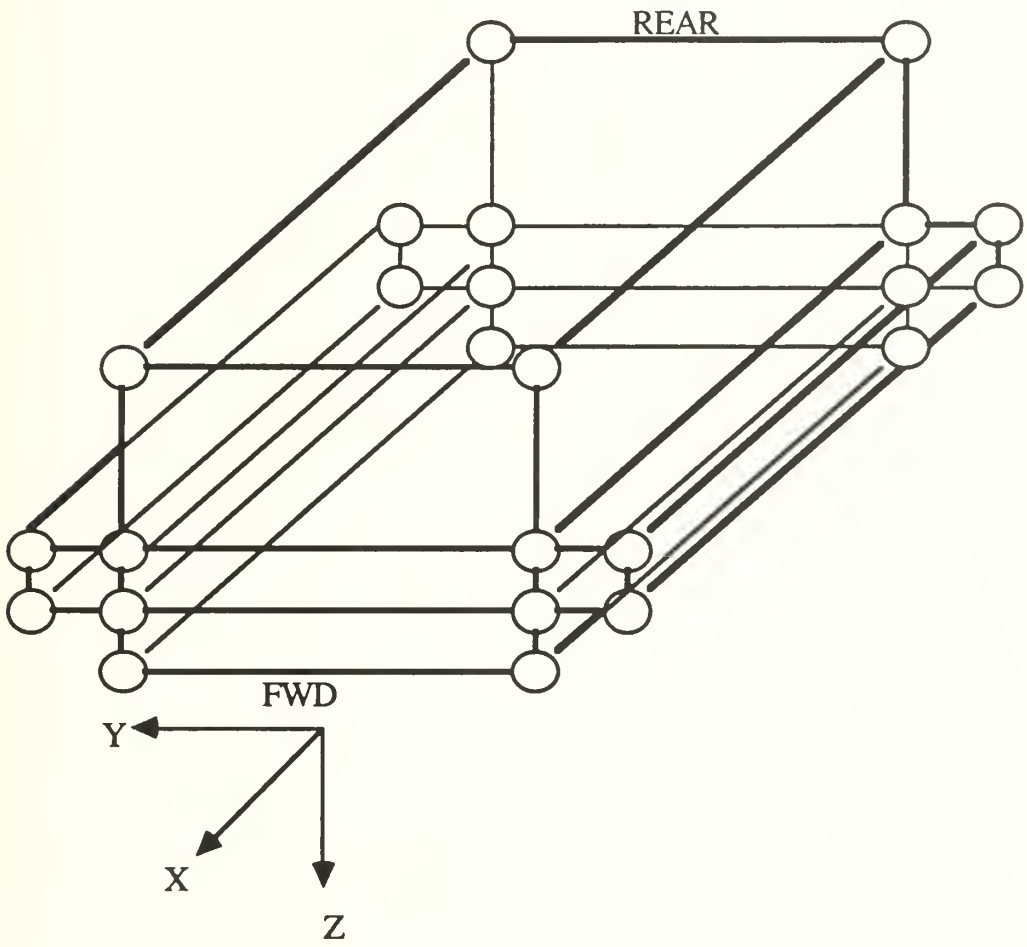

Figure 3 Center Section Wing Box Structure : Each circle represents a node of the structure. Shear sheets exist on the vertical x-z and y-z planes of each cell. Rods are represented by the lines which connect each node.

1. Summary of Field Equations

The five governing field equations are as follows:

Stress Boundary Conditions

$$\begin{bmatrix} T_x \\ T_y \\ T_z \end{bmatrix} = \begin{bmatrix} \sigma_{xx} \sigma_{xy} \sigma_{xz} \\ \sigma_{yx} \sigma_{yy} \sigma_{yz} \\ \sigma_{zx} \sigma_{zy} \sigma_{zz} \end{bmatrix} \begin{bmatrix} \nu_x \\ \nu_y \\ \nu_z \end{bmatrix} \qquad (3.1)$$

Differential Equations of Equilibr m

$$\begin{aligned} \frac{\partial \sigma_{xx}}{\partial x} + \frac{\partial \sigma_{xy}}{\partial y} + \frac{\partial \sigma_{xz}}{\partial z} + X = 0 \\ \frac{\partial \sigma_{yx}}{\partial x} + \frac{\partial \sigma_{yy}}{\partial y} + \frac{\partial \sigma_{yz}}{\partial z} + Y = 0 \\ \frac{\partial \sigma_{zx}}{\partial x} + \frac{\partial \sigma_{zy}}{\partial y} + \frac{\partial \sigma_{zz}}{\partial z} + Z = 0 \end{aligned} \qquad (3.2)$$

C nstitutive Relation

$$\begin{bmatrix} \sigma_{xx} \\ \sigma_{yy} \\ \sigma_{zz} \\ \sigma_{yx} \\ \sigma_{xz} \\ \sigma_{xy} \end{bmatrix} = \frac{E}{(1+\nu)(1-2\nu)} \begin{bmatrix} 1-\nu & \nu & \nu & 0 & 0 & 0 \\ \nu & 1-\nu & \nu & 0 & 0 & 0 \\ \nu & \nu & 1-\nu & 0 & 0 & 0 \\ 0 & 0 & 0 & 0.5-\nu & 0 & 0 \\ 0 & 0 & 0 & 0 & 0.5-\nu & 0 \\ 0 & 0 & 0 & 0 & 0 & 0.5-\nu \end{bmatrix} \begin{bmatrix} \varepsilon_{xx} \\ \varepsilon_{yy} \\ \varepsilon_{zz} \\ \varepsilon_{yz} \\ \varepsilon_{xz} \\ \varepsilon_{xy} \end{bmatrix} \qquad (3.3)$$

Strain Displacement

$$\varepsilon_{xx} = \frac{\partial u}{\partial x}$$

$$\varepsilon_{yy} = \frac{\partial v}{\partial y}$$

$$\varepsilon_{zz} = \frac{\partial w}{\partial z}$$

(3.4)

$$\varepsilon_{xy} = \frac{\partial u}{\partial y} + \frac{\partial v}{\partial x}$$

$$\varepsilon_{yz} = \frac{\partial v}{\partial z} + \frac{\partial w}{\partial y}$$

$$\varepsilon_{xz} = \frac{\partial u}{\partial z} + \frac{\partial w}{\partial x}$$

Strain Compatibility

$$\frac{\partial}{\partial z}\left(\frac{\partial \varepsilon_{yz}}{\partial x} + \frac{\partial \varepsilon_{xz}}{\partial y} - \frac{\partial \varepsilon_{xy}}{\partial z}\right) = \frac{2\partial^2 \varepsilon_{zz}}{\partial x \partial y} \qquad \frac{\partial^2 \varepsilon_{xx}}{\partial y^2} + \frac{\partial^2 \varepsilon_{yy}}{\partial x^2} = \frac{\partial^2 \varepsilon_{xy}}{\partial x \partial y}$$

$$\frac{\partial}{\partial x}\left(\frac{-\partial \varepsilon_{yz}}{\partial x} + \frac{\partial \varepsilon_{xz}}{\partial y} + \frac{\partial \varepsilon_{xy}}{\partial z}\right) = \frac{2\partial^2 \varepsilon_{xx}}{\partial y \partial z} \qquad \frac{\partial^2 \varepsilon_{yy}}{\partial z^2} + \frac{\partial^2 \varepsilon_{zz}}{\partial y^2} = \frac{\partial^2 \varepsilon_{yz}}{\partial y \partial z} \qquad (3.5)$$

$$\frac{\partial}{\partial y}\left(\frac{\partial \varepsilon_{yz}}{\partial x} - \frac{\partial \varepsilon_{xz}}{\partial y} + \frac{\partial \varepsilon_{xy}}{\partial z}\right) = \frac{2\partial^2 \varepsilon_{yy}}{\partial x \partial z} \qquad \frac{\partial^2 \varepsilon_{zz}}{\partial x^2} + \frac{\partial^2 \varepsilon_{xx}}{\partial z^2} = \frac{\partial^2 \varepsilon_{xz}}{\partial x \partial z}$$

The stress boundary conditions, Equation 3.1, relate the external traction (B.C.) to the internal stresses in the first internal layer. The second system of equations (Equation. 3.2) relates the first internal layer to

the adjacent layer by balance of internal forces; Hence it is known as the differential equation of equilibrium. Equations 3.3, the constitutive relations, convert strain uniquely into stress. Each material exhibits its own particular constitutive relationship. Aluminum behaves in an isotropic, Hookean manner. The strain displacement equations (Equations 3.4), relate the strain to the partial differential of the displacement. Finally, Equation 3.5 ensures that the second derivative of the strain is continuous or that the material will not separate anywhere within the interior. Any solution to a solid structural problem must satisfy these five sets of equations.

One approach to the problem requires the simultaneous solution of the eighteen coupled, partial differential equations (PDE) described in Equations 3.1 through 3.5. Each specific geometry of the structure and boundary condition requires a different specific solution. This method requires considerable mathematical complexity, and in fact, is frequently intractable for realistic structural configurations. The Finite Element Method (FEM) provides a general solution to a sub-geometry or element. The computer uses its high speed to solve the general case for each element. These elements may then be assembled to approximate any specific configuration of interest.

An approximate approach to this structural problem is based upon the Euler-Bernoulli assumption. This formulation assumes the functional form of the displacement, i.e., that plane sections remain plane in the structure while deforming under normal and bending loads. The assumption guarantees that the compatibility relations, Equations 3.5, are satisfied. Deformations of the structure must be small to ensure that the small angle approximation for the tangent applies (ie. less than 15 degrees of shear deformation yields an error of less than 3%). When the form of the displacement function is assumed, the solution of the eighteen PDE's reduces to a set of algebraic equations of differentials. In this case the displacement is of an assumed functional form with parameters to be determined by each specific boundary condition (B.C.) applied to the model.

This approximate approach begins by differentiating the assumed displacements using Equation 3.4.

$$v(x,y,z) = v_0 - \theta_x(y)z + \theta_z(y)x \quad (3.6)$$

$$\varepsilon_{yy} = \frac{\partial v}{\partial y} = \frac{dv_0}{dy} - z\frac{d\theta_x}{dy} + x\frac{d\theta_z}{dy} \quad (3.7)$$

The unknowns in the displacement relation become parameters to be determined. The strains are then expressed as internal stress using the constitutive relationship shown in Equation 3.3. Simplification of the axial stress expression in the y direction yields Equation 3.8.

$$\sigma_{yy} = E\varepsilon_{yy} = E\left(\frac{dv_0}{dy} - z\frac{d\theta_x}{dy} + x\frac{d\theta_z}{dy}\right) \quad (3.8)$$

Substituting these internal stress expressions into Equation 3.2 yields a set of differential equations. Equilibrating the internal stress to the boundary tractions, Equation 3.1, for a specific geometry results in a set of integral equations. The integral contains the unknown stress expressed in terms of the parameters of the assumed displacement. Equations 3.9-3.11 equate the general B.C.'s applied at wing station 65 that have an axial stress component.

$$P_y = -\int_A E\left(\frac{dv_0}{dy} - z\frac{d\theta_x}{dy} + x\frac{d\theta_z}{dy}\right) dA \quad (3.9)$$

$$M_x = -\int_A E\left(\frac{dv_0}{dy} - z\frac{d\theta_x}{dy} + x\frac{d\theta_z}{dy}\right) z\, dA \quad (3.10)$$

$$M_z = -\int_A E\left(\frac{dv_0}{dy} - z\frac{d\theta_x}{dy} + x\frac{d\theta_z}{dy}\right) x\, dA \quad (3.11)$$

From Equations 3.9-3.11, the model geometry was simplified by replacing all of the structural members by sheets that carry shear and rods that support axial loads. Through this modeling, the internal parameters become constant and can be factored outside of the integral expression.

$$P_y = -E_1\frac{dv_0}{dy}\int_A \frac{E}{E_1}\,dA + E_1\frac{d\theta_x}{dy}\int_A \frac{E}{E_1}z\,dA - E_1\frac{d\theta_z}{dy}\int_A \frac{E}{E_1}x\,dA \qquad (3.12)$$

$$M_x = -E_1\frac{dv_0}{dy}\int_A \frac{E}{E_1}z\,dA + E_1\frac{d\theta_x}{dy}\int_A \frac{E}{E_1}z^2\,dA - E_1\frac{d\theta_z}{dy}\int_A \frac{E}{E_1}xz\,dA \qquad (3.13)$$

$$M_z = -E_1\frac{dv_0}{dy}\int_A \frac{E}{E_1}x\,dA + E_1\frac{d\theta_x}{dy}\int_A \frac{E}{E_1}xz\,dA - E_1\frac{d\theta_z}{dy}\int_A \frac{E}{E_1}x^2\,dA \qquad (3.14)$$

The resulting equation was integrable since the integrand is solely related to the geometry of the cross section. The following modulus of elasticity weighted properties are defined:

$$A^* \equiv \int_A \frac{E}{E_1}\,dA \qquad (3.15)$$

$$\bar{x}^* \equiv \frac{1}{A^*}\int_A \frac{E}{E_1}x\,dA \qquad (3.16)$$

$$\bar{z}^* \equiv \frac{1}{A^*}\int_A \frac{E}{E_1}z\,dA \qquad (3.17)$$

$$I^*_{xx} \equiv \frac{1}{A^*}\int_A \frac{E}{E_1} z^2\, dA \qquad (3.18)$$

$$I^*_{xz} \equiv \frac{1}{A^*}\int_A \frac{E}{E_1} xz\, dA \qquad (3.19)$$

$$I^*_{zz} \equiv \frac{1}{A^*}\int_A \frac{E}{E_1} x^2\, dA \qquad (3.20)$$

Using these definitions, Equations 3.12-3.14 transform into:

$$P_y = -E_1 \frac{dv_0}{dy} A^* + E_1 \frac{d\theta_x}{dy} \bar{z}^* - E_1 \frac{d\theta_z}{dy} \bar{x}^* \qquad (3.21)$$

$$M_x = -E_1 \frac{dv_0}{dy} \bar{z}^* + E_1 \frac{d\theta_x}{dy} I^*_{xx} - E_1 \frac{d\theta_z}{dy} I^*_{xz} \qquad (3.22)$$

$$M_z = -E_1 \frac{dv_0}{dy} \bar{x}^* + E_1 \frac{d\theta_x}{dy} I^*_{xz} - E_1 \frac{d\theta_z}{dy} I^*_{zz} \qquad (3.23)$$

Solving for the derivatives of the displacement functions and inserting into Equation 3.8:

$$\sigma_{yy} = \frac{E}{E_1} \frac{P_y}{A^*} + \frac{E}{E_1}\left[\frac{M_z I^*_{xx} + M_x I^*_{xz}}{(I^*_{xx} I^*_{zz} - I^{*2}_{xz})}\right] x - \frac{E}{E_1}\left[\frac{M_x I^*_{zz} + M_z I^*_{xz}}{(I^*_{xx} I^*_{zz} - I^{*2}_{xz})}\right] z \qquad (3.24)$$

The differential equations have thus been transformed into a set of coupled algebraic equations. The shear stresses are solved for in a similar manner and attached in Appendix B. The general shear term is:

$$\sigma_{xy} = \sigma_{yx} = \frac{q(0)}{t} + \left[\frac{(-m_z - V_y)I^*_{yy} + (-m_y + V_z)I^*_{yz}}{(I^*_{yy} I^*_{zz} - I^{*2}_{yz})}\right]\frac{Q^*_z}{t} \qquad (3.25)$$

$$Q^*_z \equiv \int_0^{s_1} \frac{E}{E_1} y \; t \, ds \qquad (3.26)$$

$$Q^*_y \equiv \int_0^{s_1} \frac{E}{E_1} \; ds \qquad (3.27)$$

The resulting stresses for the general case are:

$$\sigma_{xx} = \frac{E}{E_1}\frac{P_x}{A^*} - \frac{E}{E_1}\left[\frac{M_z I^*_{yy} + M_y I^*_{yz}}{(I^*_{yy} I^*_{zz} - I^{*2}_{yz})}\right]y + \frac{E}{E_1}\left[\frac{M_y I^*_{zz} + M_z I^*_{yz}}{(I^*_{yy} I^*_{zz} - I^{*2}_{yz})}\right]z \qquad (3.28)$$

$$\sigma_{yy} = \frac{E}{E_1}\frac{P_y}{A^*} + \frac{E}{E_1}\left[\frac{M_z I^*_{xx} + M_x I^*_{xz}}{(I^*_{xx} I^*_{zz} - I^{*2}_{xz})}\right]x - \frac{E}{E_1}\left[\frac{M_x I^*_{zz} + M_z I^*_{xz}}{(I^*_{xx} I^*_{zz} - I^{*2}_{xz})}\right]z \qquad (3.29)$$

$$\sigma_{zz} = \frac{E}{E_1}\frac{P_z}{A^*} + \frac{E}{E_1}\left[\frac{M_x I^*_{yy} + M_y I^*_{xy}}{(I^*_{yy} I^*_{xx} - I^{*2}_{xy})}\right]y - \frac{E}{E_1}\left[\frac{M_y I^*_{xx} + M_x I^*_{xy}}{(I^*_{yy} I^*_{xx} - I^{*2}_{xy})}\right]x \qquad (3.30)$$

$$\sigma_{xz} = \sigma_{zx} = \frac{q(0)}{t} - \left[\frac{(-m_y + V_z)I^*_{zz} + (-m_z - V_y)I^*_{yz}}{(I^*_{yy} I^*_{zz} - I^{*2}_{yz})}\right]\frac{Q^*_y}{t} \qquad (3.31)$$

$$\sigma_{xy} = \sigma_{yx} = \frac{q(0)}{t} + \left[\frac{(-m_z - V_y)I^*_{yy} + (-m_y + V_z)I^*_{yz}}{(I^*_{yy} I^*_{zz} - I^{*2}_{yz})}\right]\frac{Q^*_z}{t} \qquad (3.32)$$

$$\sigma_{zy} = \sigma_{yz} = \frac{q(0)}{t} - \left[\frac{(-m_x + V_z)I^*_{zz} + (-m_z - V_x)I^*_{xz}}{(I^*_{zz} I^*_{xx} - I^{*2}_{xz})}\right]\frac{Q^*_x}{t} \qquad (3.33)$$

This system of equations can be arranged in matrix form:

$$[\sigma] = [k]\,[F] \qquad (3.34)$$

The nine generalized forces consisting of three forces, shears and moments are weighted by the k matrix to yield nine stresses. The terms that make up the non-zero elements of the matrix are listed below. The generalized k matrix follows these terms.

$$k_{11} = k_{52} = k_{93} = \frac{E}{E_1 A^*}\ ,\quad k_{18} = \frac{E}{E_1}\left[\frac{-yI^*_{yz} + zI^*_{zz}}{(I^*_{yy} I^*_{zz} - I^{*2}_{yz})}\right]$$

$$k_{19} = \frac{E}{E_1}\left[\frac{-yI^*_{yy} + zI^*_{yz}}{(I^*_{yy} I^*_{zz} - I^{*2}_{yz})}\right]\ ,\quad k_{25} = k_{45} = \frac{-I^*_{yy}}{(I^*_{yy} I^*_{zz} - I^{*2}_{yz})}\frac{Q^*_z}{t}$$

$$k_{26} = k_{46} = \frac{I^*_{yz}}{(I^*_{yy} I^*_{zz} - I^{*2}_{yz})}\frac{Q^*_z}{t}\ ,\quad k_{35} = k_{75} = \frac{I^*_{yz}}{(I^*_{yy} I^*_{zz} - I^{*2}_{yz})}\frac{Q^*_y}{t}$$

$$k_{36} = k_{76} = \frac{-I^*_{zz}\, Q^*_y}{(I^*_{yy} I^*_{zz} - I^{*2}_{yz})\, t} \quad , \quad k_{57} = \frac{E}{E_1}\left[\frac{xI^*_{xz} - zI^*_{zz}}{(I^*_{xx} I^*_{zz} - I^{*2}_{xz})}\right]$$

$$k_{59} = \frac{E}{E_1}\left[\frac{xI^*_{xx} - zI^*_{xz}}{(I^*_{xx} I^*_{zz} - I^{*2}_{xz})}\right] \quad , \quad k_{64} = k_{84} = \frac{I^*_{xz}\, Q^*_x}{(I^*_{xx} I^*_{zz} - I^{*2}_{xz})\, t}$$

$$k_{66} = k_{86} = \frac{-I^*_{zz}\, Q^*_x}{(I^*_{xx} I^*_{zz} - I^{*2}_{xz})\, t} \quad , \quad k_{97} = \frac{E}{E_1}\left[\frac{yI^*_{yy} - xI^*_{xy}}{(I^*_{yy} I^*_{xx} - I^{*2}_{xy})}\right]$$

$$k_{98} = \frac{E}{E_1}\left[\frac{yI^*_{xy} - xI^*_{xx}}{(I^*_{yy} I^*_{xx} - I^{*2}_{xy})}\right]$$

$$[k] = \begin{bmatrix}
k_{11} & 0 & 0 & 0 & 0 & 0 & 0 & k_{18} & k_{19} \\
0 & 0 & 0 & 0 & k_{25} & k_{26} & 0 & 0 & 0 \\
0 & 0 & 0 & 0 & k_{35} & k_{36} & 0 & 0 & 0 \\
0 & 0 & 0 & 0 & k_{45} & k_{46} & 0 & 0 & 0 \\
0 & k_{52} & 0 & 0 & 0 & 0 & k_{57} & 0 & k_{59} \\
0 & 0 & 0 & k_{64} & 0 & k_{66} & 0 & 0 & 0 \\
0 & 0 & 0 & 0 & k_{75} & k_{76} & 0 & 0 & 0 \\
0 & 0 & 0 & k_{84} & 0 & k_{86} & 0 & 0 & 0 \\
0 & 0 & k_{93} & 0 & 0 & 0 & k_{97} & k_{98} & 0
\end{bmatrix}$$

Further simplification is possible by applying the known loading conditions for a given boundary. For the y face at wing station 65, the sole axial load is a moment about the x-axis produced by the lift acting on the wing. Accordingly, Equation 3.24 reduces to:

$$\sigma_{yy} = \frac{E}{E_1}\left[\frac{M_x I_{xz}^*}{(I_{xx}^* I_{zz}^* - I_{xz}^{*2})}\right]x - \frac{E}{E_1}\left[\frac{M_x I_{zz}^*}{(I_{xx}^* I_{zz}^* - I_{xz}^{*2})}\right]z \qquad (3.35)$$

The profile geometry of the wing box is not quite symmetric but will be assumed so for the purpose of this calculation. Therefore the cross product of inertia terms vanish and Equation 3.35 reduces to:

$$\sigma_{yy} = \frac{-E}{E_1}\frac{M_x z}{I_{xx}^*} \qquad (3.36)$$

Similar arguments hold for the other stresses in Equations 3.28-3.33. These last two simplifications lead to an uncoupling of the algebraic expressions in the matrix as shown below:

$$k_{18} = \frac{E}{E_1}\left[\frac{z}{(I_{yy}^*)}\right] \quad , \quad k_{25} = k_{45} = \frac{-1}{I_{zz}^*}\frac{Q_z^*}{t}$$

$$k_{36} = k_{76} = \frac{-1}{I_{yy}^*}\frac{Q_y^*}{t} \quad , \quad k_{57} = -\frac{E}{E_1}\left[\frac{z}{I_{xx}^*}\right]$$

$$k_{66} = k_{86} = \frac{-1}{I_{xx}^*}\frac{Q_x^*}{t} \quad , \quad k_{93} = \frac{E}{E_1 A^*}$$

$$[k]=\begin{bmatrix} 0 & 0 & 0 & 0 & 0 & 0 & 0 & k_{18} & 0 \\ 0 & 0 & 0 & 0 & k_{25} & 0 & 0 & 0 & 0 \\ 0 & 0 & 0 & 0 & 0 & k_{36} & 0 & 0 & 0 \\ 0 & 0 & 0 & 0 & k_{45} & 0 & 0 & 0 & 0 \\ 0 & 0 & 0 & 0 & 0 & 0 & k_{57} & 0 & 0 \\ 0 & 0 & 0 & 0 & 0 & k_{66} & 0 & 0 & 0 \\ 0 & 0 & 0 & 0 & 0 & k_{76} & 0 & 0 & 0 \\ 0 & 0 & 0 & 0 & 0 & k_{86} & 0 & 0 & 0 \\ 0 & 0 & k_{98} & 0 & 0 & 0 & 0 & 0 & 0 \end{bmatrix}$$

Each stress relates to an applied boundary condition weighted by a k factor determined from the geometry of the cross section. The in-flight 1g condition generated the first load condition for the model. M_y represents the moment generated by the fuselage forward of F.S. 571 and aft of F.S. 695. For reasons of stability and equilibrium, the fore and aft moments are equal. The M_X moment is produced by the lift acting on the wing through its center of pressure, the quarter chord position on the mean aerodynamic chord. Two sets of vertical shear exist. Established by the lift on the wing, shear passes into the center section at wing station 65 acting in the negative z direction toward the top of the fuselage. The second shear results from the fuselage forward and aft of the center section wing box. This shear acts in the positive z direction at F.S. 571 and F.S. 695. P_Z accounts for the mass contained in the center section itself.

It should be noted that this solution, even with the Euler-Bernoulli assumption is tractable only for the hypothetically uniform loading where the resultant forces and moments act on the centroid of the cross-section. In fact, there exist no structural component at the centroid to carry the applied loads. Nevertheless, because of the mathematical tractability of this hypothetical case, it provides a bench mark for verifying the subsequent finite element method procedures. This idealized centroidal loading also provides the estimation of the best case analysis, i.e., the lowest possible internal structural stress for a given payload.

IV. HAND CALCULATION

In this chapter, the specific geometric properties of the P-3C aircraft are reduced to appropriate forms to be consistent with the Euler-Bernoulli formulation derived in Chapter III.

A. WING MODELING

Starting with the view from the left wingtip looking toward the fuselage, the cross sectional properties are modeled from the Structure Wing Fuselage Intersection diagram found in Lockheed Report No. 13102.

At wing station 65, a double shear splice connects the upper and lower wing surfaces to the center section wing box. Tension type splices join the beam caps together [ref 4]. At this wing station, the cross section may be modeled as a rectangle of thickness t. The outer length runs from Fuselage Station F.S. 571 to F.S. 695 or 124 inches. The inner length runs an inch shorter. The outer height and inner height are 18 and 17.5 inches respectively. The moment of inertia for this geometry is:

$$I_{xx} = \frac{1}{12}\left(b_1 h_1^{\,3} - b_2 h_2^{\,3}\right) = 5330\ \text{in}^4 \qquad (4.1)$$

The area is:

$$A = 4A_i = b_1 h_1 - b_2 h_2 = 79.5\ \text{in}^2 \qquad (4.2)$$

The distance from the centroidal axis is:

$$h3 = \sqrt{\frac{I_{xx}}{A}} = 8.19\ \text{in} \qquad (4.3)$$

The cross section transformed into rods and sheets (Figure 4).

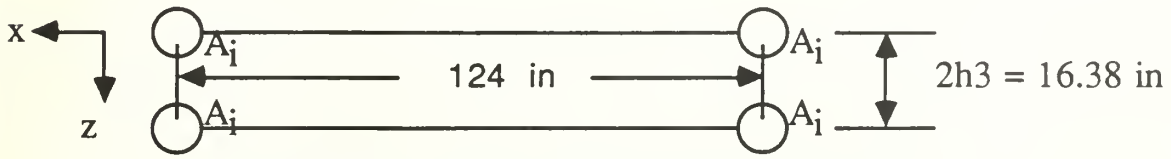

Figure 4. Wing Modeling: wing station 65

Moving towards centerline from W.S. 65, the fuselage must be accounted for in the geometry. The curved I-beams that form the main frames constitute the overwhelming majority of the additional resistance to the bending moment. This addition can be modeled as two rods located above the wing box cross section already completed and two rods at the same location as the lower part of the wing box (Figure 5).The area (A_j) represents one half of the cross sectional area of the seven frames existing between F.S. 571 and F.S. 695. A_j equals 3.5 in^2. The vertical distance (h4) from the top of the wing box to the I-beam varies in the real structure, but for simplicity will be modeled as 64.4 inches (see fuselage modeling). The distance from the wing box to the lower seven frames is z_j=2.0 inches. The new moment of inertia term is expressed in Equation 4.4.

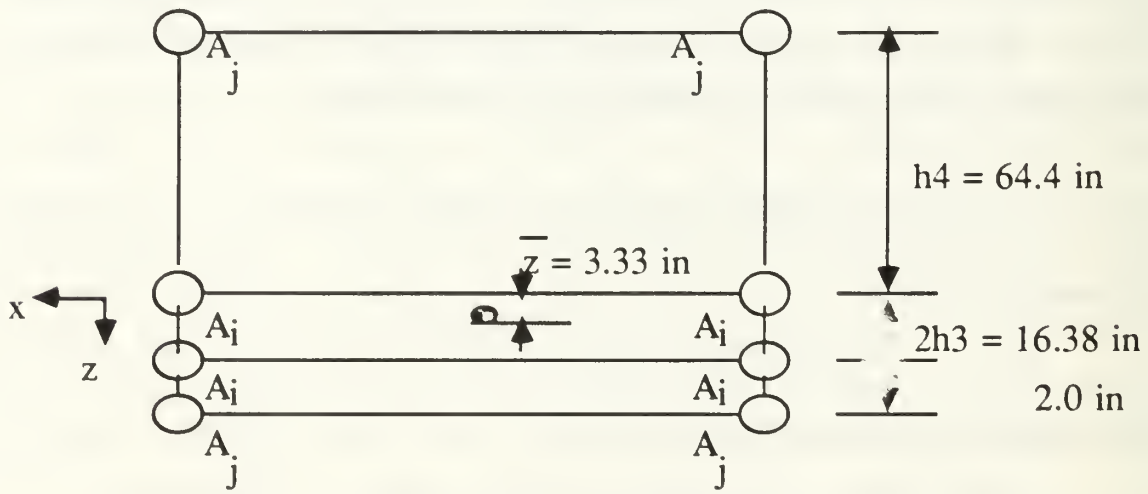

Figure 5. Wing Modeling: wing station 54

$$\bar{z}_{structure} = \frac{\left(A_{box}z_{box} + A_{curve}z_{curve} + 2A_j z_j\right)}{\left(A_{box} + A_{curve} + 2A_j\right)} = 3.33 \text{ in} \quad (4.4)$$

$$I_{xx_{total}} = I_{xx_{beam}} + z'^{2}_{beam}A_{beam} + I_{xx_{box}} + z'^{2}_{box}A_{box} + I_{xx_{low}} + z'^{2}_{low}A_{low}$$

$$I_{xx_{total}} = 0 + 32300 + 5330 + 1730 + 0 + 1160 = 40500 \text{ in}^4 \quad (4.5)$$

From Chapter III, the reduced form of the axial stress along the wing can be expressed as:

$$\sigma_{yy} = \frac{M_x z}{I_{xx}} \quad (4.6)$$

The bending moment increases by the shear loads at the W.S. 65 and those additional loads along the structure:

$$M_x(y) = M_x(65) - \int_{65}^{y} V_z(y)\, dy \quad (4.7)$$

The last term in Equation 4.7 which requires an explanation is the z location determined by the position of the member in question with respect to the modulus weighted centroid of the cross section.

The shear stress follows from the reduced form of Equation 3.26:

$$\sigma_{yz} = \frac{-V_z Q_x}{I_{xx}\ t_i} \quad (4.8)$$

The moment of inertia term was resolved for the axial stresses and will be reused here. The centroidal term from Equation 3.19:

$$Q_x = \sum_{i}^{n} \frac{E}{E_1} z_i A_i \quad (4.9)$$

As with Equation 4.7, the z_i term represents the distance between the centroid and the ith element in question. A_i represents the area of the ith element. The shear load $V_Z(y)$, increases from the wingtip to W.S. 65 as the wing generated lift dominates the weight of the structure, ordnance and fuel. Between W.S. 65 and the centerline, the shear is modified by the weight of the structure and fuel of the center section. The shears at wing stations 65 and 0 were provided by a private contractor. The data will be linearly interpolated between these two points to arrive at a shear value for a given y location.

Equation 4.8 assumes a centroidal loading which in the case of a wing with lift acting through the 30 percent chord line must be modified by the superposition of the stress due to the torsional loading. For single cell closed sections such as wing station 65, the stress expression due to torque is expressed in Equation 4.9. The enclosed area, torque and sheet thickness are included.

$$\sigma_{yz} = \frac{M_y}{2\bar{A}t} \qquad (4.10)$$

For the case of multi-cell structures refer to Allen and Haisler's text, reference 2. The authors provide a method whereby cell deformations in an n-cell structure are equated to generate n-1 equations. The final equation comes from the equilibrium expression in which the moments about the longitudinal axis are summed and equated to zero.

B. FUSELAGE MODELING:

The axial stresses in the x direction contend with the geometry shown in Figure 6.

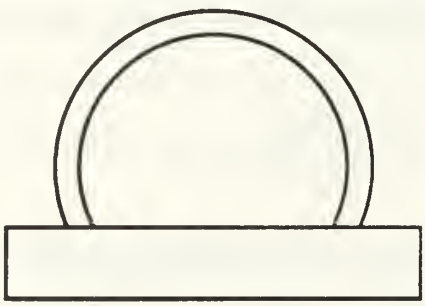

Figure 6. Simplified Fuselage Cross Section

Dissecting Figure 6 further into simpler geometries enables a component build-up approach to the section properties. Viewed from the nose of the aircraft looking back at F.S. 571, the upper shell and stringers of the fuselage may be modeled as a thin sheet (Figure 7). The center piece

may be modeled as a rectangle (Figure 8) and the lower I-beams and fuselage as two rods.

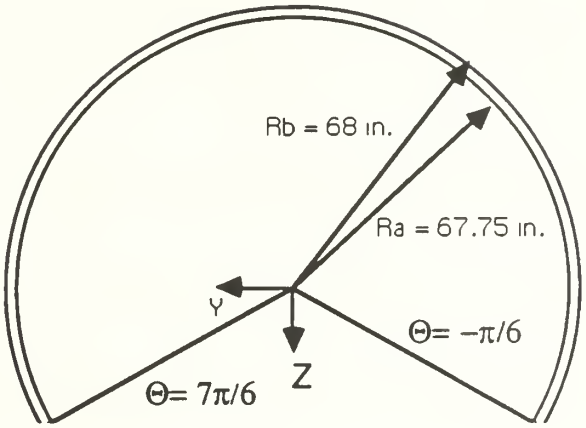

THIN SHELL MODEL

Figure 7. Upper Shell and Stringers of the Fuselage

$$A = \int_{R_a}^{R_b} \int_{\Theta=-\Pi/6}^{\Theta=7\Pi/6} r\, dr\, d\Theta = \frac{2\Pi}{3}(R_b^2 - R_a^2) = 71.2 \text{ in}^2 \quad (4.11)$$

$$\bar{z} = \frac{1}{A}\int_A z\, dA = \int_{R_a}^{R_b} \int_{\Theta=-\Pi/6}^{\Theta=7\Pi/6} (r \sin\Theta) r\, dr\, d\Theta = -28.05 \text{ in} \quad (4.12)$$

$$I_{yy_{curve}} = \int_A (\bar{z}-z)^2\, dA = \int_{R_a}^{R_b} \int_{\Theta=-\Pi/6}^{\Theta=7\Pi/6} (\bar{z} - r\sin\Theta)^2\, r\, dr\, d\Theta \quad (4.13)$$

$$I_{yy_{curve}} = 1.298\text{ E+05} - 1.120\text{ E+05} + 0.560\text{ E+05} = 7.38\text{ E+04 in}^4 \quad (4.14)$$

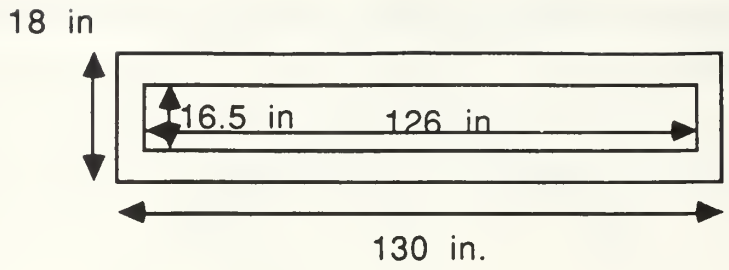

Figure 8. Center Piece of the Fuselage

$$I_{yybox} = \frac{1}{12}(b_1h_1^3 - b_2h_2^3) = 16.0\ E{+}03 \quad (4.15)$$

$$A_{box} = b_1h_1 - b_2h_2 = (18 \quad (130\ in) - (16.5in)(126in) = 261\ in^2 = 8A_i \quad (4.16)$$

The moments of inertia are computed for each piece about its respective center of gravity. At this juncture, the structure converts to rods and sheets using the computed areas and moments of inertia to calculate the vertical separation (Figure 9). An A_k of five square inches represents the area of the I-beams under the wing box and the fuselage shell lumped together two inches below the center section wing box.

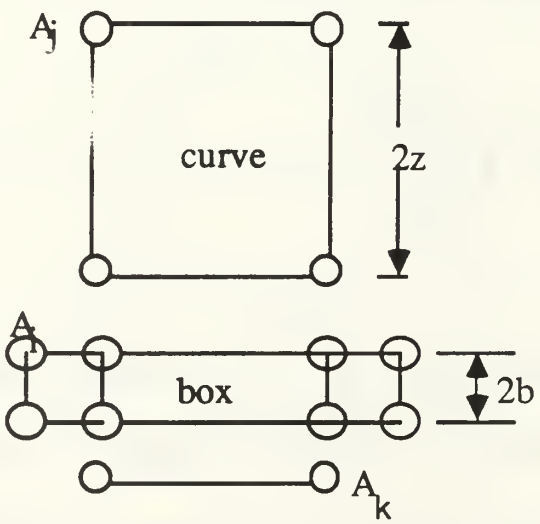

Figure 9. Idealized Fuselage Cross Section

$$z_{curve} = \sqrt{\frac{I_{yy}}{A}} = 32.19 \text{ in} \quad (4.17)$$

$$b_{box} = \sqrt{\frac{I_{yybox}}{A_{box}}} = 7.83 \text{ in} \quad (4.18)$$

Solving for the modulus weighted center of gravity for the entire cross section enables the section moment of inertia to be calculated. Figure 10 shows the dimensions of interest for the complete cross section.

$$\bar{z}_{structure} = \frac{\left(A_{box}z_{box} + A_{curve}z_{curve} + 2A_k z_k\right)}{\left(A_{box} + A_{curve} + 2A_k\right)} = 0.65 \text{ in} \quad (4.19)$$

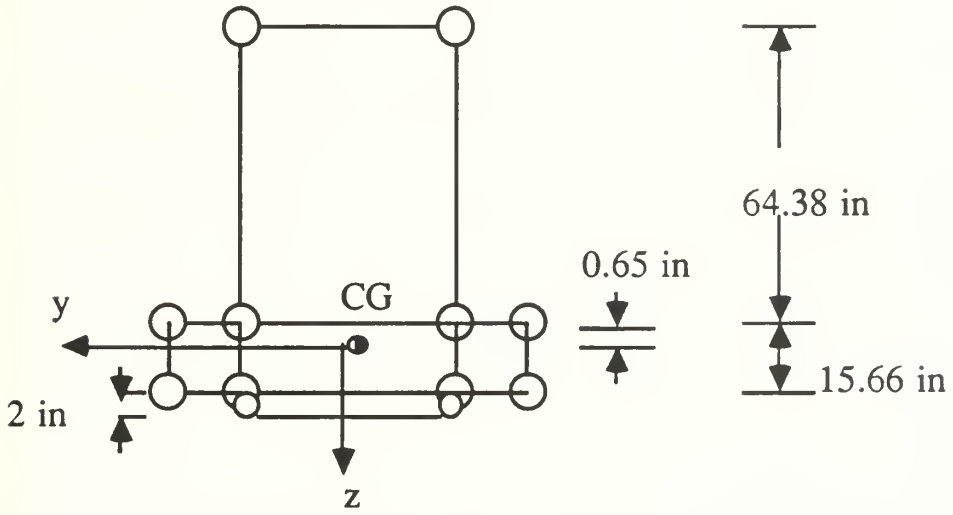

Figure 10. Idealized Fuselage Cross Section : with dimensions

$$I_{yytotal} = I_{yycurve} + z'^{2}_{curve}A_{curve} + I_{yybox} + z'^{2}_{box}A_{box} + I_{yylow} + z'^{2}_{low}A_{low} \quad (4.20)$$

$$I_{yytotal} = 7.38 \text{ E+04} + 7.68 \text{ E+04} + 1.60 \text{ E+04} + 1.34 \text{ E+04} + 0 + 0.29\text{E+04}$$

$$= 1.83 \text{ E+05 in}^4 \quad (4.21)$$

The simplified x direction axial stress equation follows:

$$\sigma_{xx} = \frac{M_y z}{I_{yy}} \quad (4.22)$$

The moment of inertia term has just been solved for the homogeneous case in Equation 4.21. The location of the bar in question, referenced to the modulus weighted centroid, determines the value of z. The boundary conditions at F.S. 571 and 695 were developed in the boundary condition section and calculated in Appendix A. To determine the moment at a particular fuselage station between F.S. 571 and 695 requires a similar calculation based upon this component build up method.

The shear stress for the face at F.S. 571 simplifies from Equation 3.24:

$$\sigma_{xz} = \frac{V_z Q_y}{I_{yy}\, t_i} \quad (4.23)$$

The terms in Equation 4.23 follow directly from the explanation for Equation 4.10 where:

$$Q_y = \sum_i^n \frac{E}{E_1} z_i A_i \quad (4.24)$$

The moment of inertia term was previously solved for in Equation 4.20. The thickness depends upon the location of interest. The shear force V_Z was calculated for F.S. 571 in Appendix A. All of the 1g boundary condition loads are shown in Figure 11.

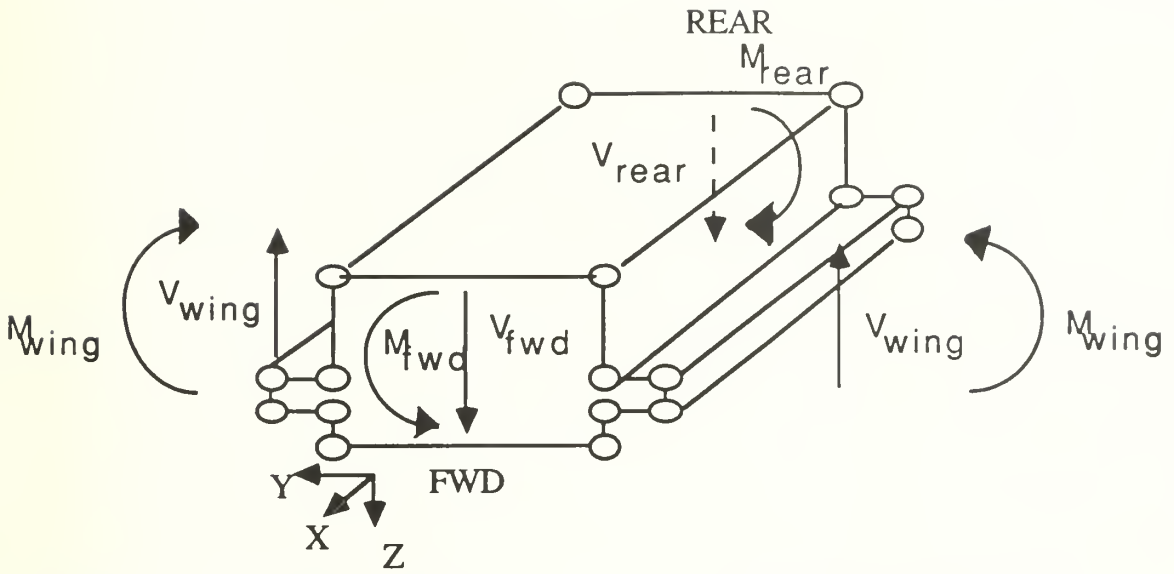

M_{wing} = 5.97E+06 in-lbs

M_{rear} = 3.31E+06 in-lbs

M_{fwd} = 3.31E+06 in-lbs

V_{wing} = 24,400 lbs

V_{rear} = 8,700 lbs

V_{fwd} = 12,600 lbs

Inertia = $2^{*} V_{wing} - V_{rear} - V_{fwd}$ = 27500 lbs

Figure 11 Boundary Condition Loads for Center Section Wing Box : at 1g.

In this chapter, the actual P-3C aircraft geometry is reduced to idealized rods and rectangular sheets which are statically equivalent to the actual load and moment carrying capacity of the aircraft. The actual load and moments are reduced to centroidal boundary conditions as shown in Figure 11 for the 1 g condition. Stresses calculated from the 1 g condition can be simply scaled to any multiple for feasibility studies.

V. FINITE ELEMENT METHOD

The finite element method provides a direct solution to the field equations (as described in Chapter II) without the simplification of Euler-Bernoulli hypothesis. For the center section wing box it can provide improved accuracy over the hand calculated solution for centroidal loading as well as for other more realistic cases which are beyond hand calculations. Small or finite elements are solved in the general sense to simultaneously satisfy the eighteen field equations. These building blocks are subsequently combined and matched to form the structure or geometry of interest. Equilibrium must be satisfied at each node where the elements connect. The external displacement and force boundary conditions are applied to the structure. The solution to this combination of elements and boundary conditions satisfies the minimum energy principle. This principle guarantees a unique solution which minimizes the strain energy preserved in the structure as it deforms under loading. Model One was constructed to compare this method of calculation to that accomplished by hand calculations with centroidal boundary conditions. (See Appendix D for FEM examples)

Upon verification, subsequent load conditions can be constructed to model a flight condition of interest (i.e. 3g, 3.5 g . . . etc.). The resulting internal stresses will identify locations which require redesign. Modified configurations (i.e. fuel/payload) cause a redistribution of the inertial loads within the center section. This model provides the tool from which to explore these modifications to determine their effect on the internal stresses of the wing box structure. If critical stresses are identified, the model lends itself to study the replacement options for the structure. Redesign options include additional area/mass added to a component or, on the other hand, part replacement with an alternative material (i.e. different composites). Both of these options require assessable software modifications to the model definition.

The model to be constructed for finite element analysis is not geometrically identical to the actual structure of the P-3C aircraft. A

geometrically exact model would be too complex to implement and too time consuming to execute; it is appropriate only for the actual design stage. A geometrically simplified model retaining the pertinent structural features is constructed herein; its application is intended for problem identification and assessment of different options of payload, distribution structural enhancement and modifications.

The finite element software used in this investigation is the PAL2 V 4.0 by MacNeil Swindler Corp. This software can be run on PC class of computers, it has provisions for analysis of composite materials and can be executed under NASTRAN on mini and mainframe class of computers.

This chapter describes the geometric definition of the model and the software related procedures to assure the appropriateness of the finite element method implementations.

A. PROCEDURES

1. Geometric Definition

The nodal points that describe the structure of interest are defined using a rectangular coordinate system (polar and spherical are available). Once the nodes are in place and the material specified (i.e. 2014 T-4 aluminum), the elements that make up the structure are connected to the nodal lattice. Rods join two nodes together while quadrilateral plates connect four nodes. The circular rods are defined by inner and outer diameter. The shear area is nothing more than a correction term for the parabolic shear distribution across the beam face. The square bar shear area equals the cross-sectional area divided by 1.2. Their lengths are prescribed by the lattice. The shear plate thickness is specified, while the node locations determine the planer dimensions. The relation of this model to the actual structure is shown in Figure 1 and Figure 12 below.

2. Boundary Conditions

The PAL2 software accepts forces, pressure loads, line loads, and concentrated moments. This software limitation requires the boundary condition moments and shears to be distributed by means of a hand calculation. The calculated shear and moment loads apply indirectly to the

nodes on the boundary of interest via a dummy structure that when coupled with the Saint-Venant principle generates the centroidal load conditions on the center section boundaries. This last procedure is necessitated by the need to generate centroidal loads to validate the hand calculations. Once the model has been validated, non-centroidal loads may be applied to develop a complete structural response envelope given a variety of inertial load conditions. Once an inertial load is specified for a given flight condition, the structure is equilibrated; Displacements and rotations specified as zero at one node will prevent it from flying off into space.

3. Model One

The first model built contains the rod and sheet structure used in the hand calculation (see Figure 12). The model sizing comes directly from the hand calculation with one exception. The wing box thickness was modified to accommodate the lattice structure. A compromise height of sixteen inches required a slight adjustment (less than 1 part in 40) to the rod cross sectional areas. This adjustment maintained constant moment of inertia terms I_{xx} and I_{yy}. The node locations/model dimensions are listed in Appendix C. The bar diameters were taken directly from the hand calculation A_i and A_j terms except where they are altered to account for the change in wing box thickness. For simplicity, the shear plate thickness was uniformly chosen as 0.25 inches.

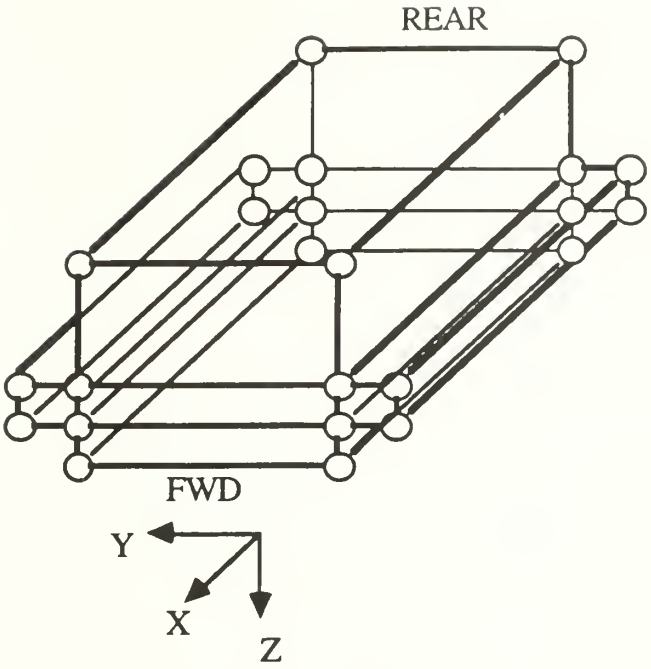

Figure 12. Center Section Wing Box Structure : model one (bars and sheets)

Modeling the hand calculated centroidal load requires a dummy structure built from the face of the center section on each of its four boundaries. This dummy structure enables the centroidal loads to be applied at the boundary by means of the Saint-Venant principle in which only the nonequilibrated loads are transmitted through the structure. These nonequilibrated loads transform to the centroidal loads as they propagate away from the boundaries.

At wing station 65 for example, the rectangular cross section consists of four nodes. This plane is repeated two times in both the positive and negative y-direction as depicted in Figure 13. There are a total of four sheets on the y faces and eight each on the x and z faces of the dummy structure. Rods connect each pair of adjacent nodes. The hand calculation sizes the rod diameter. The loads applied outboard of wing station 65 are such that at the boundary of interest they become the centroidal loads identical to those used in the hand calculation. The four nodes on the positive y face of the resulting structure have their displacements set to zero to ensure equilibrium throughout the structure.

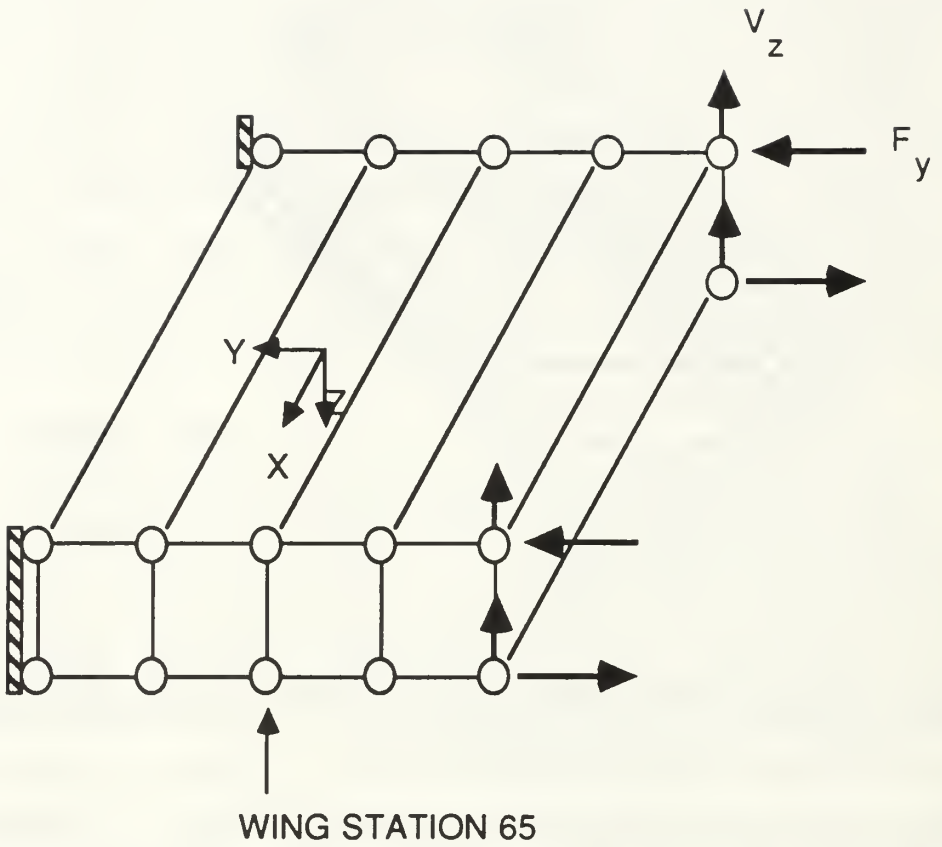

Figure 13. Wing Station 65 Boundary : modeled for comparison with hand calculations

The remaining three boundaries are modeled in a parallel manner using the dummy structure to achieve a centroidal loading on the boundary of interest for direct comparison to the hand results.

The verifications of model formulation and implementations are made against a hand calculated bench mark model for the simplified centroidal loading conditions (described in Chapter II). The results are described in Appendix D. They are well within the theoretical expectations and the model presented herein can be considered as fully verified; it can be used for feasibility studies, operational envelope definition and structural design tradeoffs.

VI. ALTERNATIVE SOLUTIONS (PROBLEM EXTENSION)

This chapter discusses the limitations of verifying the finite element solution with the hand calculated results to the boundaries of the structure for a 1g centroidally distributed load. Extensions from these verified boundary results explore the full range of the finite element solutions and their applicability to the existing center section wing box problem. The solution range encompasses all of the loads discussed in Chapter II.

A. BENEFITS OF THE DUAL APPROACH

The usefulness of the combined solution method falls into two categories. The first lies in the verification of the centroidal boundary condition (or lower bound) stresses for the finite element method. It should be pointed out that the results of the hand calculation are valid only for the boundaries of the model. This limitation lies in the generation of the boundary condition loads. The loads are generated external to the wing box and do not account for any distribution of inertia loads within the center section itself. Secondly, completion of the finite element modeling enables a rapid solution to the altered boundary conditions associated with a 3g load for a 95,000 pound zero fuel weight P-3 with 60,000 pounds of fuel (the original configuration of interest). Since the solution varies within the center section as the inertial loads are redistributed, several may be applied simulating any of a number of configuration options. The most straightforward is an equitable distribution throughout the center section. From this original problem, design options are explored which will satisfy the structural requirements associated with the proposed payload growth.

1. Configuration Change

A configuration change to the P-3H short of a structural modification requires that a solution to the altered boundary condition loads be applied to the existing finite element model. The internal stresses are solved using the available software. The new fuselage boundary condition loads are calculated in the same manner as those calculated in

Appendix A. For the case of increasing the zero fuel weight, additional lift must be generated by the wings to sustain this extra mass at the 3g flight condition. The second solution found in Chapter II under wing boundary condition loads, provides a component build up method to calculate the new moments and shears at wing station 65.

a. Example 1

Suppose a new ESM suite at SS3 adds 100 pounds to the work station 100 inches forward of F.S. 571. The 3g flight condition requires an additional 300 pounds of lift out of the wings distributed along the span. This addition alters the moment and shears at wing station 65. Fuselage station 571 would experience an additional 300 pounds of shear and 30,000 in-pounds of bending moment. These new loads are added to the existing boundary condition loads and a solution generated. The internal stresses may then be examined for failure determination. In the case where no overstress has occurred then the inertia loads within the center section may be redistributed until the limiting stresses are reached.

2. Changing Material Properties

There exist three solutions to the problem load which exceeds the yield stress of a given structure given constant center section inertia forces. The first two alternatives increase the moment of inertia terms (denominator of Equations 3.21-3.26) thereby reducing the internal stress. Either additional material may be used to increase the cross section (i.e. fortify existing sections) or the dimensions of the wing box and/or fuselage must be increased. The more appealing third option from the weight viewpoint involves the use of a material with a greater specific strength.

Replacing the entire aluminum structure with a single material (i.e. composite) fails to alter the internal stresses. Rather, the yield stress of the structure increases enabling greater loads to be safely carried. The partial use of stronger materials in high stress locations of the wing box would solve the structural problem for the case in which only portions of the structure exceeded the yield stress.

a. Example 2

Changing the load requirements from 3.0 to 3.5 g's provides another opportunity to observe the structural limits. The problem requires that the 3.5 g boundary load conditions for the wing and fuselage stations be calculated. As a rudimentary approach, the 3 g loads are multiplied by the ratio (3.5/3.0). The new loads are applied to the boundaries of the computer model and the stresses checked. Exceeding the yield stress anywhere in the structure requires a redesign by one of the three methods mentioned above. Assuming that only the stress in the axial bars between wing station 65 and the fuselage are excessive they will be targeted with composite replacement. The aluminum will be replaced by a composite material with a simple software modification. The new model will be run against the 3.5g boundary condition loads to complete the process. The new internal stresses within the member can now be analyzed, and further modifications made if necessary.

Two extensions from the original verified finite element solution are explored. The first discusses the problems associated with payload increase consisting of a single piece of equipment, while the latter confronts the issues surrounding an increase in the flight envelope of the aircraft. Both extensions demonstrate design benefits of the verified finite element solution for the purpose of answering the structural integrity question associated with the payload increase.

VII. RESULTS

This chapter examines the internal stresses of the P-3C center section wing box for the two calculation methods that were employed in the analysis. The hand calculations are based upon the Euler-Bernoulli assumption that plane sections remain plane. The finite element method simultaneously satisfies the field equations for a given element from which the internal stresses are determined. The results compare a 1g centroidal boundary load condition (ie. lower bound).

Comparison of the stresses is limited to wing station 65L and fuselage station 571. Similar results are expected for the other two boundaries. The right wing boundary condition is symmetric to the left. Fuselage Station 695 has a scaled down shear force while its cross-section is identical to the forward section. .

The results are presented graphically (Figures 16 and 17) and followed in tabular form (Tables 7.1 through 7.4). Figures 14 and 15 depict the internal stress locations for F.S.571 (X-face) and W.S.65L (Y-face).

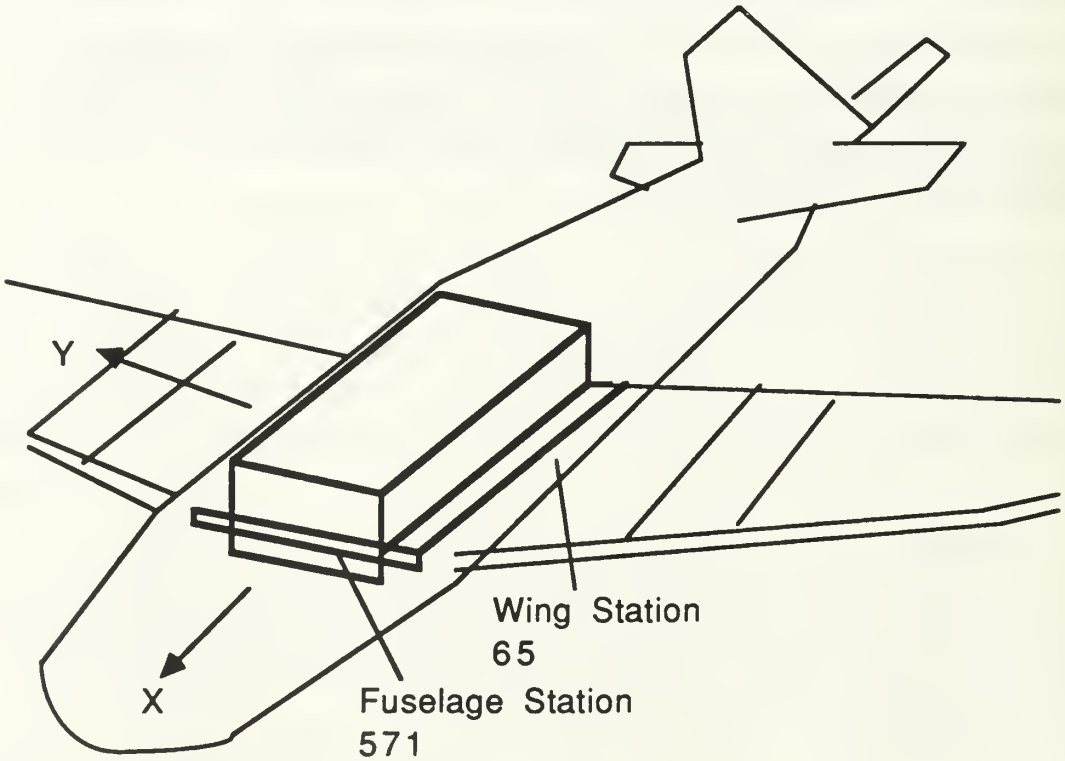

Figure 14. Stress Locations

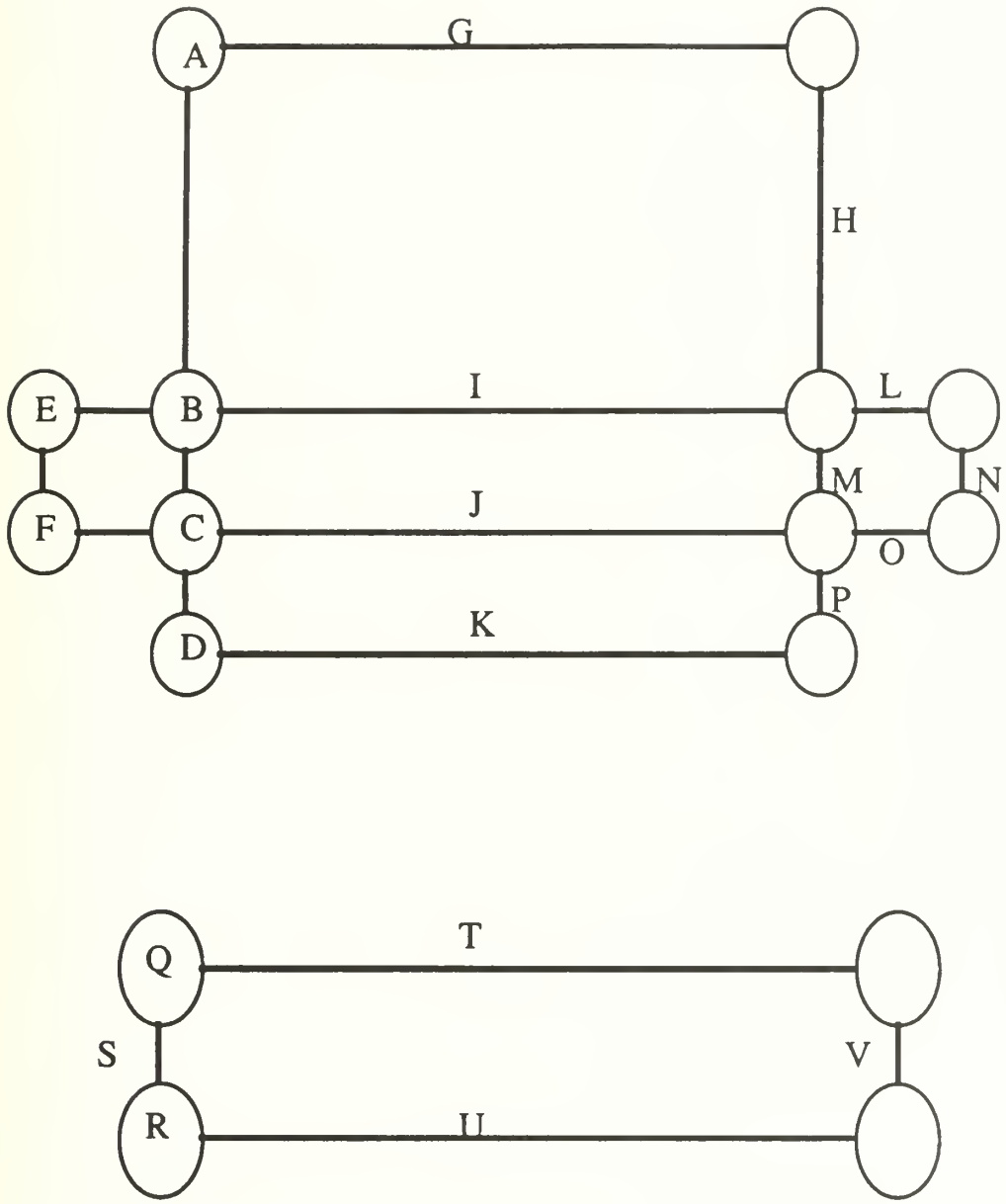

Figure 15. Stress Identification : X face(top) Y face(bottom)

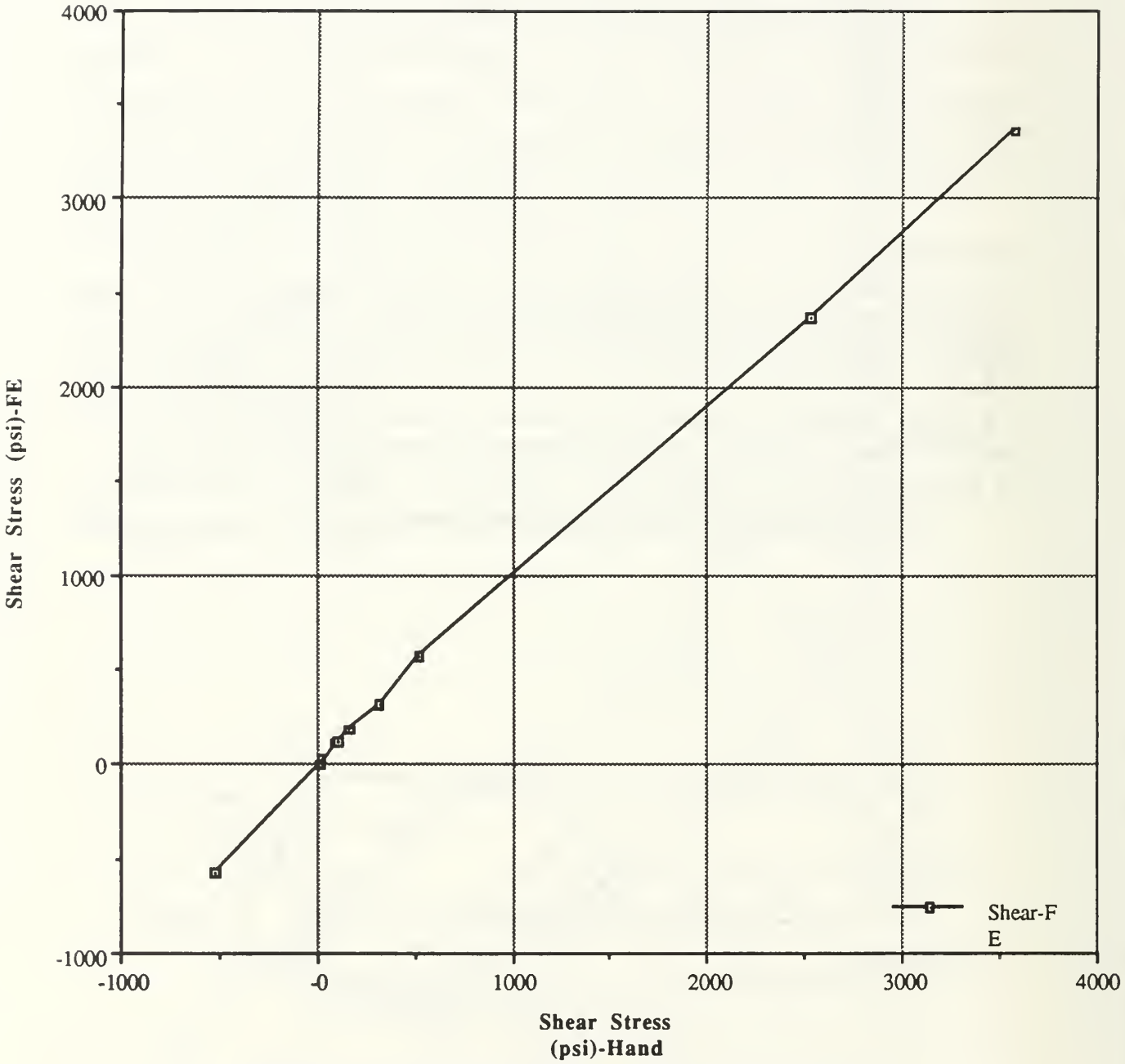

Figure 16. Graph of Shear Stress Results

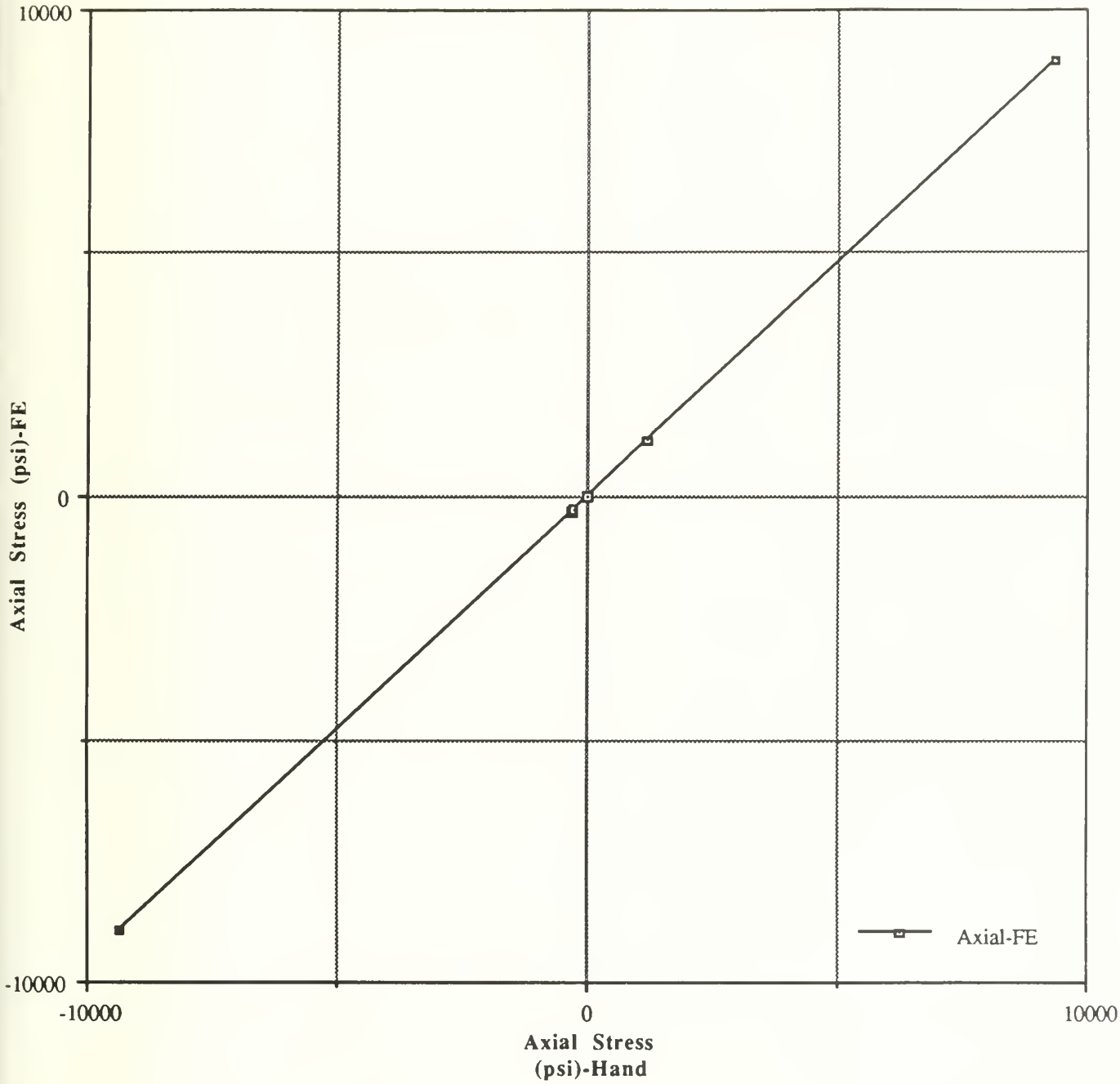

Figure 17. Graph of Axial Stress Results

TABLE 7.1. X Face Axial Stress

Axial Stress	FEM (psi)	Hand Calc (psi)
A	1159	1176
B	-5.5	11.8
C	-294	-278
D	-333	-314
E	-4.9	11.8
F	-294	-278

TABLE 7.2. X Face Shear Stress

Shear Stress	FEM (psi)	Hand Calc (psi)
G	0	12
H	313	315
I	0	24
J	0	16
K	0	15
L	108	95
M		165
N		100
O	12.5	21
P	28	23

TABLE 7.3. Y Face Axial Stress

Axial Stress	FEM (psi)	Hand Calc (psi)
Q	8932	9355
R	-8932	-9355

TABLE 7.4. Y Face Shear Stress

Shear Stress	FEM (psi)	Hand Calc (psi)
S	3361	3568
T	-569	-518.5
U	569	518.5
V	2369	2531

The stresses on the X-face of the model result from an application of a 12,566 pound shear force 260 inches from the boundary of interest. This load results in the correct shear and moment at F.S.571 due to the Saint-Venant effect. With this centroidal loading of the fuselage, the stresses in the horizontal sheets are expected to be zero. The hand calculation leaves small finite stresses due mainly to round off in the five by five matrix solution. The finite element method predicts the stress as zero. The finite element axial stress in member A tends toward the high side, while the remaining rod stresses tend toward the low. This phenomenon results from the centroidal axis of the finite element model shifting towards the top of the fuselage since the area of the shear sheets are included.

The shear load applied at thirty-three percent chord combined with the force couple realistically models the aerodynamic loads on the wing. The finite element stresses on this face are all within ten percent of the hand calculated results.

The finite element stresses agree favorably with the hand results, well within twenty percent. Axial stresses tended to be closer to the predicted hand results than did the shear stresses. The Euler-Bernoulli assumption explains the difference between the two sets of results.

These results verify the finite element model. The extension from this problem remains to run the model using a realistic 3g load condition for a 95,000 pound zero fuel weight aircraft with 60,000 pounds of fuel. Since the fuel and internal loadout are never constant, the inertia loads within the center section must be varied to develop a full range of solutions for the center section wing box.

VIII. SUMMARY, CONCLUSIONS AND RECOMMENDATIONS

The Navy is considering the feasibility of increasing the patrol aircraft P-3C zero fuel weight enabling avionics and payload growth. This analysis examines the consequences to the structural requirements of the center section wing box. Specifically, the investigation provides an analytical means with which to explore the structure given a payload increase of 18,000 pounds.

Two solutions to the structures field equations are investigated: a simplified hand solution for preliminary feasibility calculations and a more precise solution for design analysis. Together, the solutions provide a necessary check for the results. The hand calculations calibrate the finite element solution on the boundary of interest. These calculations are valid only for the extremely simplified centroidal loading. This loading gives rise to uniformly distributed forces and moments and hence, the best case (lower bound stress) condition. The primary purpose of the hand calculation is to identify the existence of any structural problems on the wing box boundary and to assure the correctness of the finite element method model. This assurance is especially important when the computer generated model is used to explore different options of payload redistribution feasibility studies, operation envelope definition and structural design tradeoffs.

The extension remains to utilize the finite element model for various load conditions combining the boundary shears and moments together with several inertial distributions representative of the limiting flight envelope. The critical center section components are to be identified and redesigned from the wing box feasibility studies which, in turn, will lead to an optimized solution. The options will include structural fortification, composite reinforcement, substitution, and inertial distribution limitations within the center section.

At this stage, finite element output is limited to stress and deformation data. Software options are also available to generate dynamic responses which are needed for flutter characterization.

This analytical package facilitates the generation of design points for the replacement center section wing box. Successful implementation of the product will provide the technical basis for RFP generation.

APPENDIX A. BOUNDARY CONDITIONS

A. P-3C FUSELAGE WEIGHT BREAKDOWN

(Weights from P-3C specification 1983)

COMPONENT		WEIGHT(LBS)	
TAIL		1965	
WING		9095	
	WING		7595
	C.S.		1500
PROPULSION		15041	
NACELLE		4877	
LANDING GEAR		3666	
	MAIN		3055
	NOSE		611
AIR COND./ANTI-ICE		2022	
	WING		800
	NOSE		322
	C.S.		800
	REAR		100
FLIGHT CONTROLS		1509	
	WING		750
	C.S.		600
	REAR		159
ELECTRICAL		1813	
	WING		500
	C.S.		1313
INSTRUMENTS		477	
HYDRAULIC		433	
BODY		9973	
	NOSE		4773
	C.S.		1200
	REAR		4000

APU		514	
ELECTRONICS GROUP		10376	
	NOSE		3376
	C.S.		6000
	REAR		1000
ARMAMENT		1404	
FURNISHINGS		3830	
	NOSE		2000
	C.S.		330
	REAR		1500
PHOTO		89	
		67,084	

B. SHEAR AND MOMENTS BY SECTION

1. Nose -- Loads at F.S. 571

COMPONENT	WEIGHT (LBS)	MOMENT-ARM (IN)	MOMENT (10^5 IN-LB)
INSTRUMENTS	477	350	1.66
BODY	4773	275	13.10
APU	514	283	1.45
ELECTRONICS GP	3376	200	6.75
ARMAMENT	404	100	0.40
FURNISHINGS	2000	300	6.00
AIR COND. /ANTI-ICE	322	470	1.51
PHOTO	89	470	0.42
NOSE GEAR	611	300	1.83

SHEAR = 12566 LBS MOMENT = 3.31 * 10^6 IN-LBS @ 1g

SHEAR = 37698 LBS MOMENT = 9.93 * 10^6 IN-LBS @ 3g

2. Rear -- Loads at F.S. 695

COMPONENT	WEIGHT (LBS)	MOMENT-ARM (IN)	MOMENT (10^5 IN-LB)
TAIL GP	1965	505	9.92
BODY	4000	250	10.00
FURNISHING	1500	200	3.00
FLIGHT CONTROLS	159	300	0.48
ELECTRONICS	1000	100	1.00
AIR COND. /ANTI-ICE	100	400	0.40

SHEAR = 8724 LBS MOMENT = 2.48 * 10^6 IN-LBs @ 1g

SHEAR = 26172 LBS MOMENT = 7.44 * 10^6 IN-LBS @ 3g

EQUILIBRIUM REQUIRES NOSE & AFT MOMENT EQUAL
THEREFORE ASSUME DIFFERENCE IN MOMENTS COMES FROM ELEVATOR FORCE .

ELEVATOR MOMENT = 0.83 * 10^6 IN-LBS

3. Center Section

COMPONENT	WEIGHT (LBS)
HYDRAULIC	433
ELECTRICAL	1313
FLIGHT CONTROLS	600
BODY	1200
ELECTRONICS GP	6000
ARMAMENT	1000
FURNISHINGS	330
AIR COND. /ANTI-ICE	800
WING	1500

CENTER SECTION WEIGHT = 13176 LBS @ 1g, 39528 LBS @ 3g

C. WING LOADS

(Provided by Aerostructures Inc.)

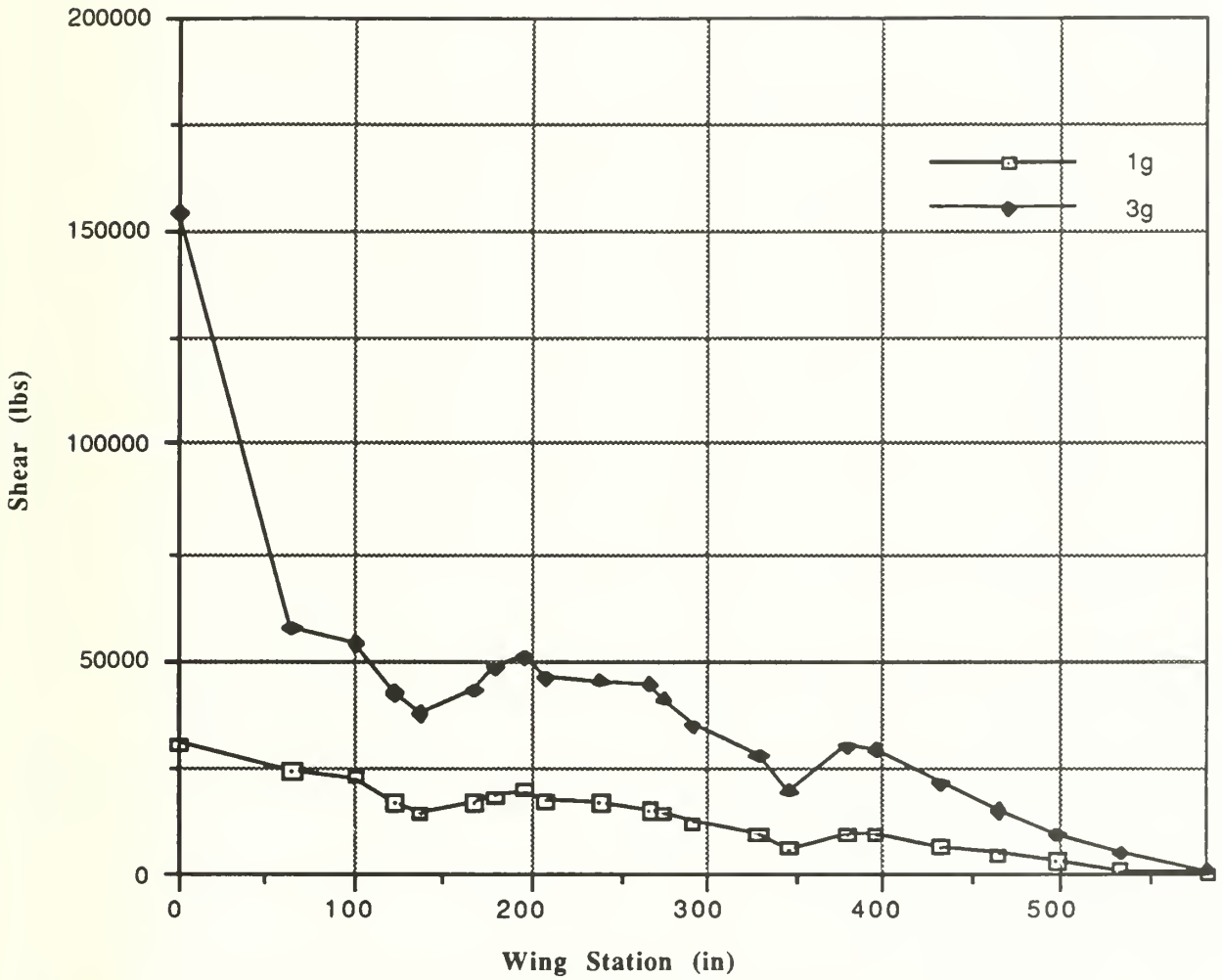

Figure 18. P-3C Wing Shear : 135,000 pounds gross weight.

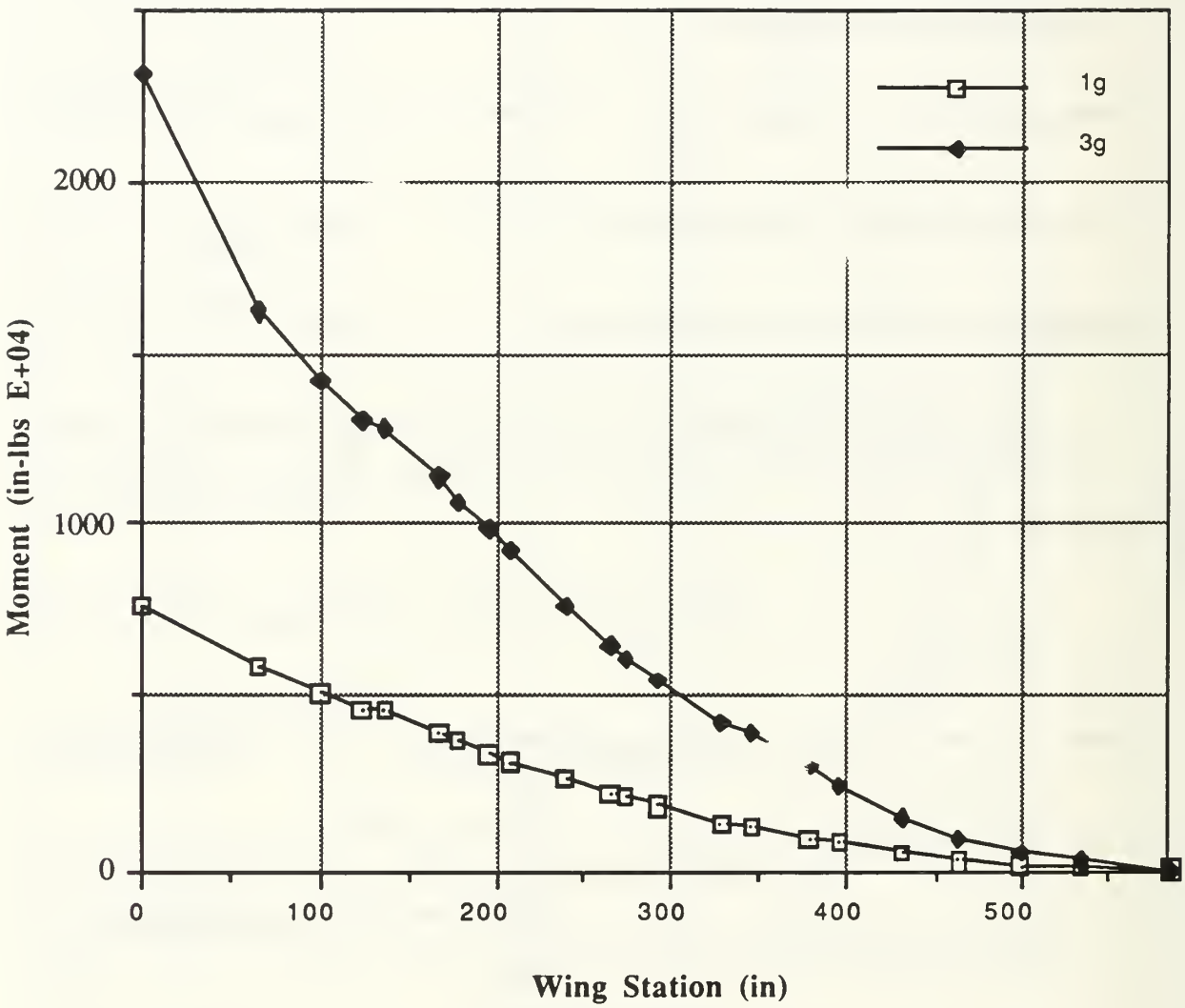

Figure 19. P-3C Wing Moment : 135,000 pounds gross weight.

APPENDIX B. GENERAL SHEAR SOLUTION

The following argument follows directly from Reference 1.

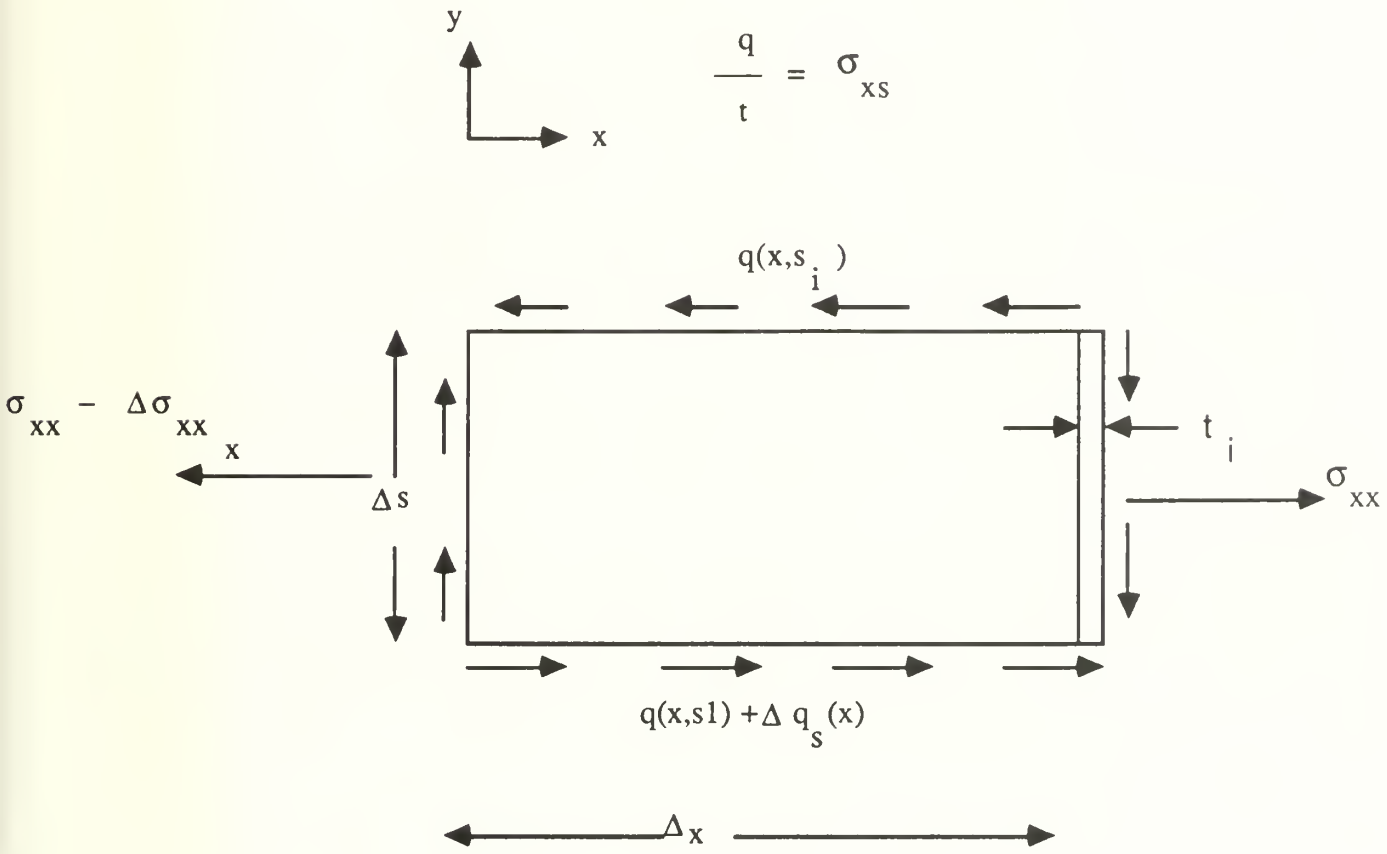

Solving for the shear begins with summing the forces in the x direction:

$$\sum F_x = 0 \quad \text{(B.1)}$$

$$0 = \int_{s_1}^{s_1+\Delta s} \sigma_{xx}\, t(x_0,s)\, ds - \int_{s_1}^{s_1+\Delta s} (\sigma_{xx}-\Delta\sigma_{xx})[t(x_0,s)-\Delta t_x(s)]\, ds + \int_{x0-\Delta x}^{x0} q(x,s_1)+\Delta q_s)\, dx - \int_{x0-\Delta x}^{x0} q(x, s_1)\, dx \quad \text{(B.2)}$$

Cancelling like terms and dividing by $\Delta s \Delta x$ Equation B.2 simplifies to:

$$0 = \frac{1}{\Delta s}\int_{s_1}^{s_1+\Delta s} \sigma_{xx}\frac{\Delta t_x(s)}{\Delta x}\,ds + \frac{1}{\Delta s}\int_{s_1}^{s_1+\Delta s} \frac{\Delta \sigma_{xx_x}}{\Delta x} t(x_0,s)\,ds +$$

$$\frac{1}{\Delta x}\int_{x0-\Delta x}^{x0} \frac{\Delta q_s(x)}{\Delta s}\,dx - \frac{1}{\Delta s}\int_{s_1}^{s_1+\Delta s} \Delta\sigma_{xx_x}\frac{\Delta t_x(s)}{\Delta x}\,ds \quad (B.3)$$

Since the thickness does not vary along the length of the sheet those terms fall out of the expression leaving:

$$\frac{dq}{ds} = -t(x_0,s)\frac{\partial \sigma_{xx}}{\partial x} \quad (B.4)$$

Integrating both sides of of Equation B.4 yields:

$$q(s_1) = q(s=0) - \int_0^{s_1} t\frac{\partial \sigma_{xx}}{\partial x}\,ds \quad (B.5)$$

Substituting the general expression for axial stress (σ_{xx}) developed in the earlier solution into Equation B.5 produces:

$$q(s_1) = q(s=0) - \int_0^{s_1} \frac{\partial}{\partial x}\{ -\frac{E}{E_1}[\frac{M_z^* I_{yy}^* + M_y^* I_{yz}^*}{(I_{yy}^* I_{zz}^* - I_{yz}^{*2})}]y + \frac{E}{E_1}[\frac{M_y^* I_{zz}^* + M_z^* I_{yz}^*}{(I_{yy}^* I_{zz}^* - I_{yz}^{*2})}]z \}t\,ds \quad (B.6)$$

Applying symmetry to the geometry removes the cross product of inertia terms. Taking the partial derivative with respect to x yields:

$$q(s_1) = q(s=0) - \int_0^{s_1} \{ \frac{\partial M_z E}{\partial x E_1} [\frac{1}{I^*_{zz}}] y + \frac{\partial M_y E}{\partial x E_1} [\frac{1}{I^*_{yy}}] z \} t \, ds \quad (B.7)$$

$$\frac{\partial M_z}{\partial x} \equiv -m_z(x) - V_y(x) \quad (B.8), \qquad \frac{\partial M_y}{\partial x} \equiv -m_y(x) + V_z(x) \quad (B.9)$$

Substituting the definitions from Equation B.8 &9 into B.7 and neglecting the distributed moments for the given 3g loading condition results in:

$$q(s_1) = q(s=0) - \int_0^{s_1} \{ \frac{E}{E_1} [\frac{-V_y(x)}{I^*_{zz}}] y + \frac{E}{E_1} [\frac{V_z(x)}{I^*_{yy}}] z \} t \, ds \quad (B.10)$$

For a given location of x the shears are constant and may be removed from the integral along with the moments of inertia. Employing the definitions from Equation B.11&12, Equation B.10 reduces to:

$$Q^*_z \equiv \int_0^{s_1} \frac{E}{E_1} y \, t \, ds \quad (B.11), \qquad Q^*_y \equiv \int_0^{s_1} \frac{E}{E_1} z \, t \, ds \quad (B.12)$$

$$q(s_1) = q(s=0) - \frac{V_y(x)}{I^*_{zz}} Q^*_z - \frac{V_z(x)}{I^*_{yy}} Q^*_y \quad (B.13)$$

Assuming the shear (Vy) produced by a rudder deflection and experienced at F.S. 695 is negligible, equation B.13 reduces to:

$$q(s_1) = q(s=0) - \frac{V_z(x)}{I^*_{yy}} Q^*_y \quad (B.14)$$

APPENDIX C. NODAL POINT LOCATIONS FOR FEM

A. FEM OF FUSELAGE BOUNDARY CONDITION

1. Fuselage Boundary Modeling

nodal point locations 1
1, 0, 54, -72 through 5, 527, 54, -72
6, 0, -54, -72 through 10, 527, -54, -72
11, 0, 54, -8 through 15, 527, 54, -8
16, 0, -54, -8 through 20, 527, -54, -8
21, 0, 54, 8 through 25, 527, 54, 8
26, 0, -54, 8 through 30, 527, -54, 8
31, 0, 54, 10 through 35, 527, 54, 10
36, 0, -54, 10 through 40, 527, -54, 10
41, 0, -63, -8 through 45, 527, -63, -8
46, 0, -63, 8 through 50, 527, -63, 8
51, 0, 63, -8 through 55, 527, 63, -8
56, 0, 63, 8 through 60, 527, 63, 8
blank line
c bars are all circular cross-sections
c quad plates are all shear members 1/4 inch thick
c 2024-T4 aluminum material
material properties 10.5E6, 0, 2.59E-4, 0.33,40E3
c X dir rods
beam type 3 4.76 0
element generate 21
1 5 10 1 5 0
blank line
beam type 3 6.31 0
element generate 21
51 55 45 1 10 0
56 60 50 1 10 0
21 25 30 1 5 0
blank line
beam type 3 7.90 0

```
element generate 21
11 15 20 1 5 0
blank line
beam type 3   2.52   0
element generate 21
31 35 40 1 5 0
blank line
c     Y dir rods
beam type 3   2.12   0
element generate 21
1 5 10 1 5 1
31 35 40 1 5 1
blank line
beam type 3   5.15   0
element generate 21
45 20 16 25 1 0
20 15 11 5 1 0
15 55 51 40 1 0
50 30 26 20 1 0
30 25 21 5 1 0
25 60 56 35 1 0
blank line
c     Z dir rods
beam type 3   2.12   0
element generate 31
1 5 10 40 1 5 10 2
blank line
beam type 3   1.78   0
element generate 31
41 45 55 60 1 10 5 2
blank line
quad plate element  3  0  0.25
element generate 31
1 5 10 40 1 5 10 0
1 5 10 40 1 5 10 1
```

1 5 10 40 1 5 10 2
41 45 55 60 1 10 5 1
blank line
do connect 26 46 41 16 through 30 50 45 20 step 1 1 1 1
do connect 21 56 51 11 through 25 60 55 15 step 1 1 1 1
element generate 21
16 20 45 1 25
26 30 50 1 20
51 55 15 1 40
56 60 25 1 35
blank line
end definition

2. Fuselage Load Conditions

c load condition for fuselage station 571-1g St Venant forces and moments applied 1
fz 2094 5 10 15 20 25 30
blank line
displacements applied 1
ta 0.0 16
tx 0.0 1 6 11 21 26 31 36 41 46 51 56
tz 0.0 1 6 11 21 26 31 36 41 46 51 56
blank line
solve
quit

B. FEM OF WING BOUNDARY CONDITIONS

1. Wing Boundary Modeling

c wing station 65 shear loads located at 33% chord
nodal point locations 1
1 0 -60 0
2 80 -60 0
3 0 -60 16
4 80 -60 16

```
17   0 -70  0
18  80 -70  0
19   0 -70 16
20  80 -70 16
blank line
nodal point locations 31
1 2 4 20 1 2 4
blank line
c    all beams have circular cross section
c    quad plates are all shear members 1/4 inch thick
c    2024-T4 aluminum material
material properties 10.5E+06, 0, 2.59E-4, 0.33, 40E+03
beam type 3   5.04   0
element generate 31
1 2 4 20 1 2 4 2 0
blank line
beam type 3   1.38   0
element generate 31
1 2 4 20 1 2 4 0 0
1 2 4 20 1 2 4 1 0
blank line
quad plate element  3  0  0.25
element generate 31
1 2 4 20 1 2 4 0
1 2 4 20 1 2 4 1
1 2 4 20 1 2 4 2
blank line
end definition
```

2. Wing Load Conditions

```
c    wing box centroidal loading lift line at 33% chord
forces and moments applied 1
fy   1.828E+05   19 20
fy  -1.828E+05   17 18
fz  -5064            17 19
```

```
fz   7136              18 20
fx   5184              17 18
fx  -5184              19 20
blank line
displacements applied 1
ta  0.0 1 2 3 4
blank line
solve
quit
```

APPENDIX D. FINITE ELEMENT IMPLEMENTATIONS

Appendix D outlines the procedures necessary to correctly model a structure using the finite element method. The first portion discusses the modeling elements and is followed by an explanation of displacement and equilibrium force boundary conditions. Application of the Saint-Venant Principle to modeling centroidal force distributions completes the topic. Examples which highlight these issues are supported with numerical results and summarized.

The first decision that one must make when modeling a structure lies in choosing the correct elements. Rods and sheets constitute the model for the hand calculation. The PAL2 software provides four beam type elements and two quadrilateral plate elements from which to select. The first sheet element provides resistance to bending, axial and shear loads. In resisting bending and axial loads, this element impedes relative displacement motion between the nodes that surround it. Another way to state this behavior is that the element stiffens the k matrix. The second sheet type resists only shear loads. Since the plate elements do not resist relative motion between the surrounding nodes, this plate must be surrounded by beam elements as a picture is surrounded on its four sides by a frame. Beam 4 models an anti-symmetric cross sectional element. Beam 3 models a rod with circular cross section. The user defines the inner and outer rod diameter. The program automatically calculates the remaining geometric properties from this information including the shear area. The shear area represents a fictitious area that corrects for the parabolic shear distribution across the face of an element. For a circular rod, the shear area equals the cross sectional area divided by 1.185. Beam 2 creates a rectangular cross section which varies in height and width along its length. Beam 1 generates a constant area cross section member. In addition to the area, the user must specify the torsional moment of inertia, the moments of inertia, the shear area, and the distance from centroid to the most distant point on the cross sectional area. The shear area correction factor for a square cross section beam is 1.20. Curved beam elements are also available but not used since

the hand model was constructed from straight rods to facilitate calculation.

The second area of interest lies in displacement boundary conditions; how to tie the structure down in space to prevent that unequilibrated shear of 10^{-7} pounds from driving the structure into the computer abyss. If six degrees of freedom were eliminated from one location on the structure, would the tie down affect the internal stresses? To illustrate this point, four circular rods of one square inch cross section (beam type 3) surround a 100 square inch shear plate of the second type discussed above. The left two nodes have their x, y and z translations set to zero while a shear force of unity in the negative z direction is applied to the upper right hand node. The reaction forces are calculated at the left end by the software. These reaction forces are applied to the left end with the same shear load while the displacement boundary conditions are eliminated from the left end and three translations and rotations are set to zero on the lower right hand node of the structure. The reaction forces calculated at the lower right hand node for this second case are eleven orders of magnitude less than the applied load while the internal stresses are unchanged in all five elements. Similar results are obtained for an example extended into the third dimension. The results from this exercise enable the center section wing box to be tied down at one node since it too is in static equilibrium. With confidence one knows that there will be insignificant stresses generated within the modeled structure due to the displacement boundary condition.

Finally, the St. Venant principle must be addressed when applying boundary condition loads and displacements. Unequilibrated loads are transmitted through the body while equilibrated loads dissipate quickly as they extend through the structure. From the modeling aspect this affects the manner in which one exerts forces on the structure. If large single point forces are applied at a few nodes around the structure, this practice may lead to the finite element solution being driven to an alternate form.

Consider a hollow square beam forty inches in length (figure 20). The beam consists of four cubes of eight nodes each whose faces in the longitudinal direction are absent while the remaining four faces are made from shear plates (type 2) 1/10 inch thick. Circular rods of five square inch cross sections connect the longitudinal edges of the forty inch beam. Square beams of 1/100 square inch cross sections surround the remaining

sides of the quadrilateral plate elements. The small dimension of the secondary beams enable a blending with the sheets. The four left end nodes of the long beam are attached with three translational degrees of freedom set to zero. The right end has a shear load of unity applied to the upper node nearest the observer. The manner in which one applies the load determines the form of the solution taken by the finite element method. If the load is applied as described above, the right end panel nearest the observer will display a shear of 0.984 psi. Observation of the output stresses five inches from the right end of the long beam reveals that the beam is in static equilibrium. Results from the hand calculation predict a value of 0.750 psi.(see Allen and Haisler p221). However, if the shear load above is redistributed to the centroid as a shear and moment with one quarter of each divided among the four end nodes, the expected solution of 0.742 psi results or one percent variation from the hand calculated solution. Static equilibrium is satisfied by this solution at the same location described above. In practice, loads should be distributed as evenly about the structure as possible.

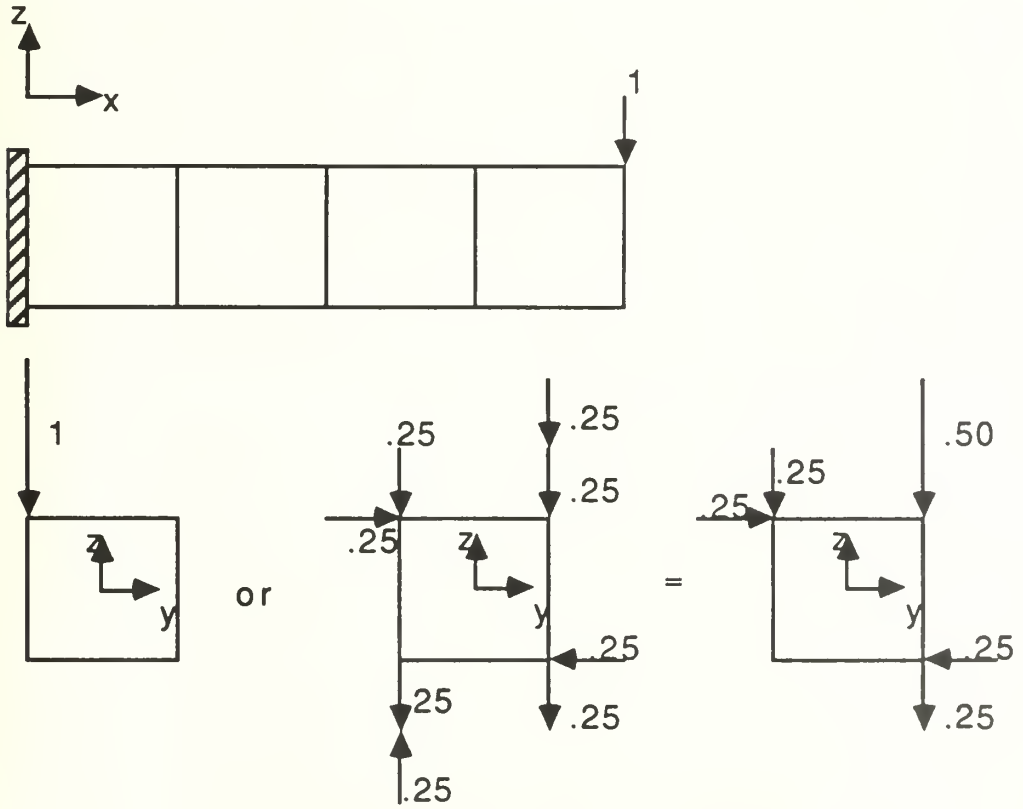

Figure 20. Square Beam Model

For the case in which the boundary condition loads are not perfectly matched to the internal stresses, Saint-Venant points out that the structure requires space to enable the equilibrated forces to dissipate. As an extension of the previous problem, consider a similar beam consisting of twelve cubes of which five are shown in Figure 21. The first plane of interest lies 1/8 th of the distance from the loaded end to the wall. The end cube of the beam is subdivided from one to two sheets per face (case a), from two to four (case b), and from four to six (case c). The increased number of end nodes facilitates the application of a more evenly distributed superposition of shear and moment loads to the beam in comparison to the previous example. The results of the three plar are compared t> the hand calculations for each of the three conditions shown in Figure 21. Figure 22 shows the loading for cases a and b. Case c distributes the load in a similar fashion among sixteen nodes.

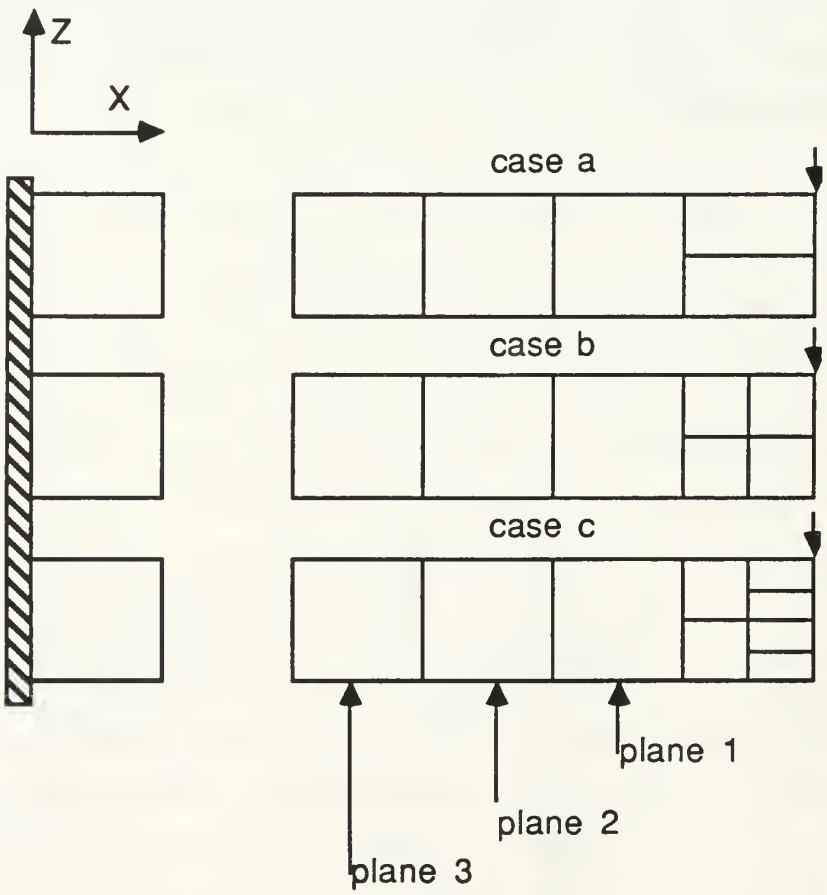

Figure 21. Twelve Cube Beam

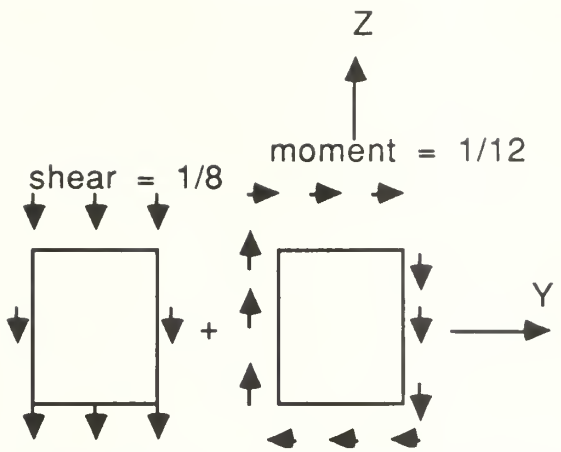

Figure 22. Load Conditions : superposition of shear and torsion loads as seen from end view of case a and case b.

A. SUMMARY

In Figure 23 the observer is viewed from the negative z axis from the wall. In Figures 24, 25, and 26, τ_1 is located in the upper right-hand corner, $-\tau_2 = \tau_4$ is in the lower left corner, and τ_3 is in the center.

The stresses in plane 1 (Figure 24) vary by as much as forty percent from the hand results while by plane 2 (Figure.25) the variation drops dramatically to 5.6 percent. The stress difference in plane 3 (Figure.26) reduces further to 3.2 percent. As the distance from the boundary condition increases from plane 1 to plane 3, the finite element stresses approach the hand calculations thereby validating the Saint-Venant principle.

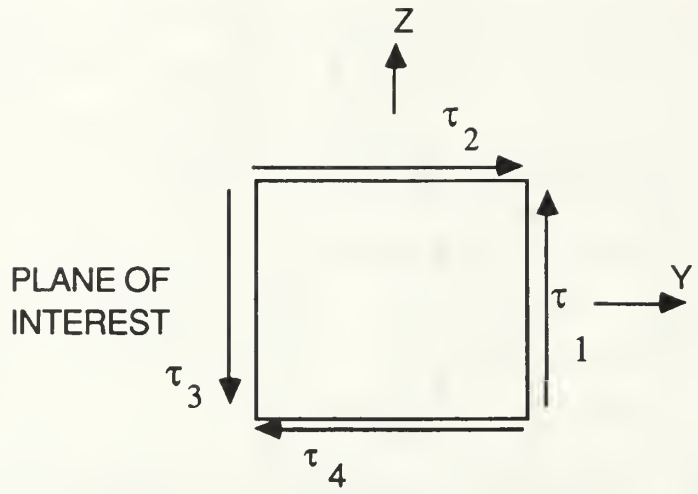

Figure 23. Axial View of Example Beams

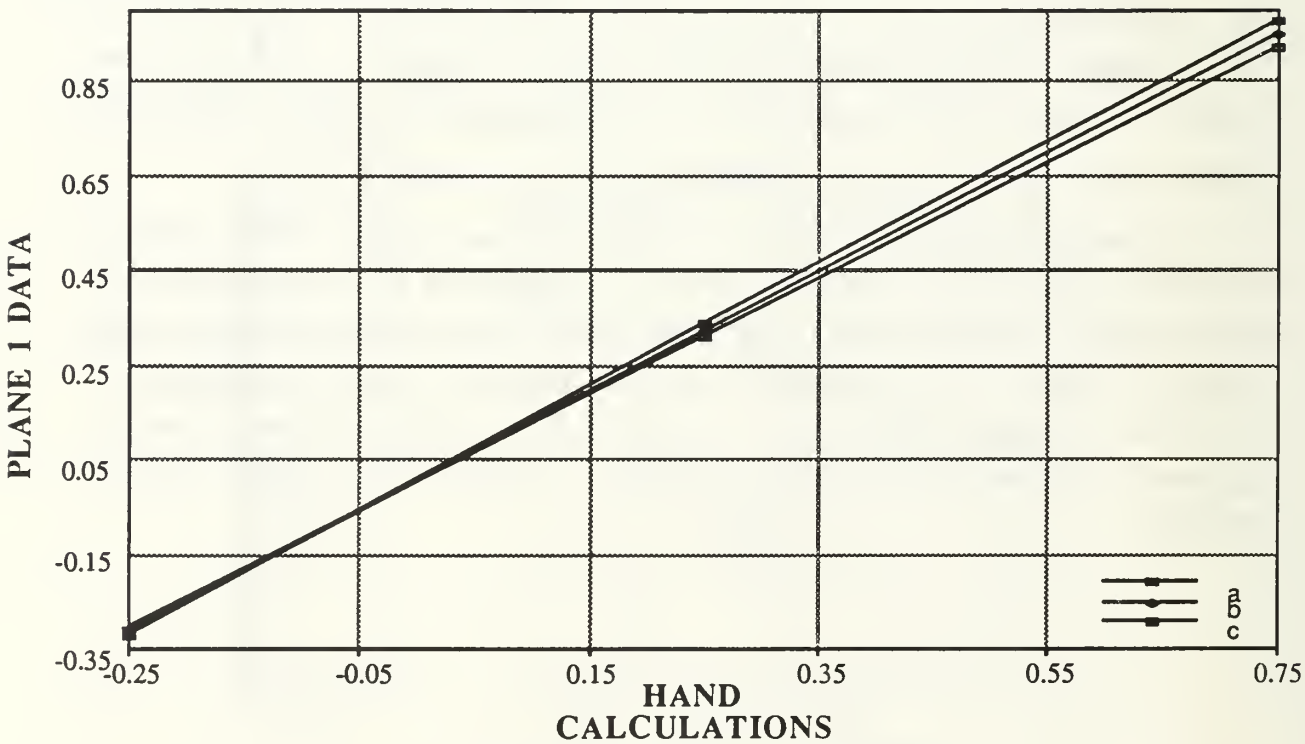

Figure 24. Plane 1 Results

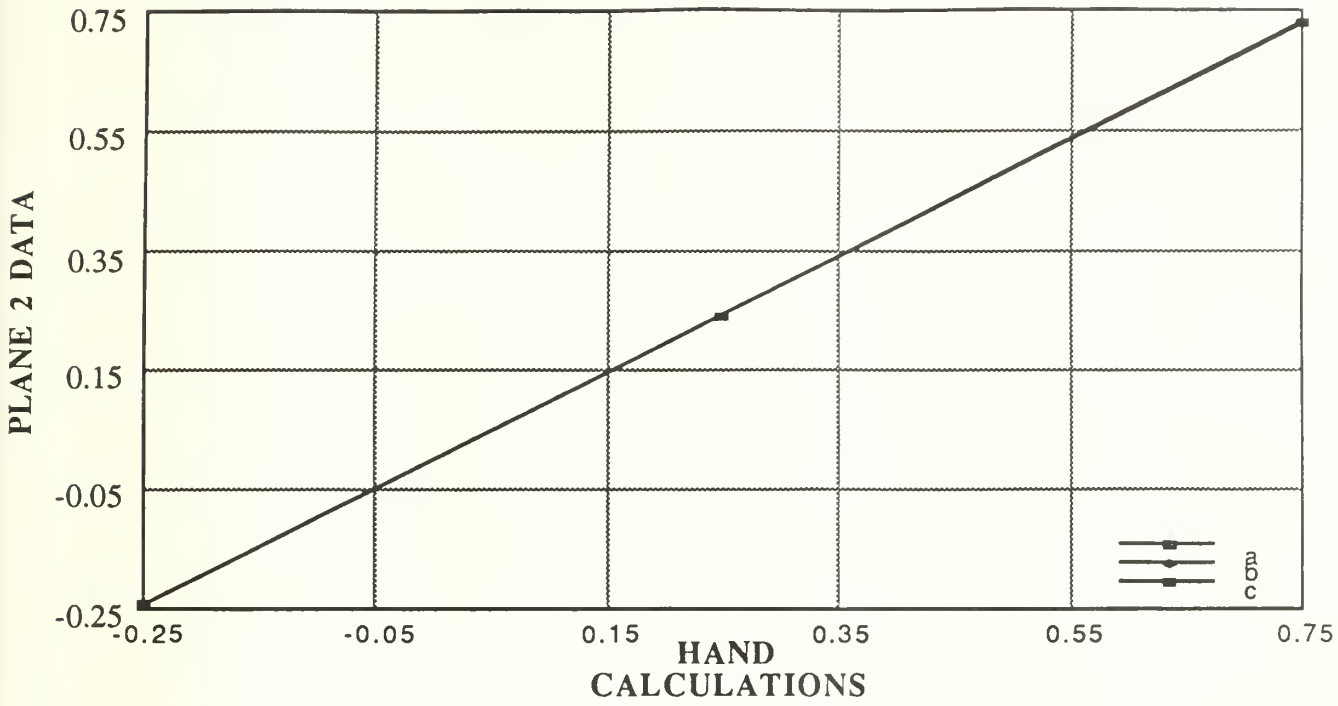

Figure.25. Plane 2 Results

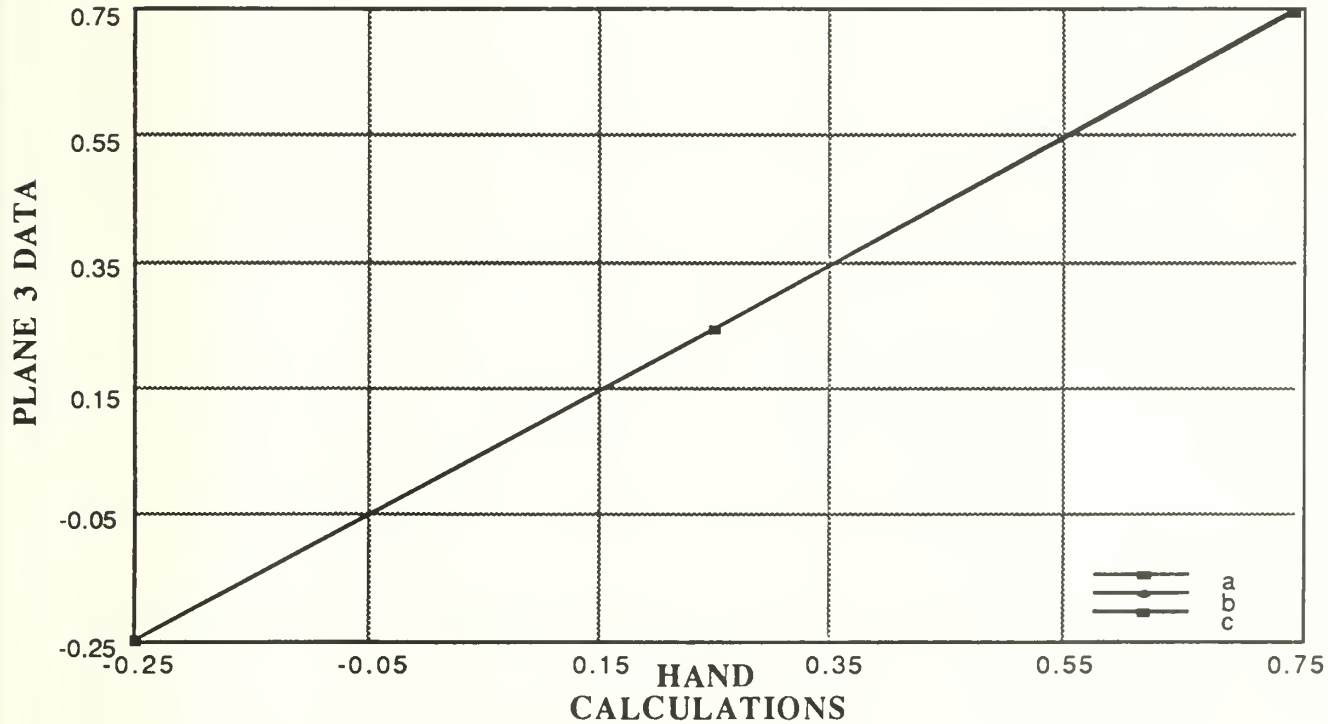

Figure 26. Plane 3 Results

As an extension of these example problems to the center section wing box, dummy structural area must be located between the boundaries of the structure and the applied loading conditions. This area will ensure that the proper shear stresses are retrieved from the structure as occurred in moving from plane 1 to plane 2 above. The moments of the applied loading condition must be modified to account for the added distance through which they must act.

These results which compare hand calculations (using the Euler-Bernoulli assumption) to those of the finite element method illustrate the importance of correctly modeling the boundary conditions to minimize their effect on the results. In addition, "dummy extended space" facilitates the location of centroidally distributed loads through the Saint-Venant Principle.

LIST OF REFERENCES

1) Interview between Mr. Nam Phan, Naval Air Systems Command, Monterey, Ca, and the author, 12 October 1990.

2) Allen, David H. and Haisler, Walter E., Introduction to Aerospace Structural Analysis, John Wiley and Sons Inc., New York, 1985.

3) Lockheed Report 13102.

4) Phone conversation between A. Anderjaska, Aerostructures, Inc, Arlington Va, and the author, 18 October 1990.

5) Detail Specification for P-3C Airplane ASW Four Engine Fiscal Year 1982 Procurement.

6) Cook, Robert D., Malkus, David S., and Plesha, Michael E.,Concepts and Applications of Finite Element Analysis 3rd Edition, John Wiley and Sons Inc., New York, 1989.

INITIAL DISTRIBUTION LIST

1. Defense Technical Information Center 2
   Cameron Station
   Alexandria, Virginia 22304-6145

2. Library, Code 52 2
   Naval Postgraduate School
   Monterey, California 93943-5100

3. Aeronautical Engineering Curricular Office, Code 31 1
   Naval Postgraduate School
   Monterey, California 93943

4. Professor Edward M. Wu, Code 31 4
   Department of Aeronautical Engineering
   Naval Postgraduate School
   Monterey, California 93943

5. Lt. Steven D. Culpepper 2
   C/O C.A. Barreca
   6 Aspetuck Hill Lane
   Weston, Connecticut 06883

6. E. R. Wood, Chairman 1
   Department of Aeronautics and Astronautics
   Naval Postgraduate School
   Monterey, California 93943-5000

7. RADM R. W. West Jr., Superintendent 1
   Naval Postgraduate School
   Monterey, California 93943-5000

8. Commander, Naval Air Systems Command (AIR-5114B) 1
   Washington, D. C. 20361-9320
   Attn: CDR E. Boington

9. Commander, Naval Air Systems Command (AIR-5302) 1
   Washington, D. C. 20361-9320

Thesis
C92575
c.1

Culpepper
Structural considerations for aircraft payload modification-P-3H zero fuel weight increase.